EFFECTS OF Nb_2O_5 ADDITION ON THE FORMATION AND PROPERTIES OF THE Bi-BASED SUPERCONDUCTORS

A THESIS SUBMITTED TO
THE GRADUATE SCHOOL OF NATURAL AND APPLIED SCIENCES
OF
MIDDLE EAST TECHNICAL UNIVERSITY

BY

NADER GHAZANFARI

IN PARTIAL FULFILMENT OF THE REQUIREMENTS
FOR
THE DEGREE OF MASTER OF SCIENCE
IN
PHYSICS

AUGUST 2006

Approval of the Graduate School of Natural and Applied Sciences

_____

Prof. Dr. Canan Özgen
Director

I certify that this thesis satisfies all the requirements as a thesis for the degree of Master of Science.

_____

Prof. Dr. Sinan Bilikmen
Head of Department

This is to certify that we have read this thesis and that in our opinion it is fully adequate, in scope and quality as a thesis for the degree of Master of Science.

_____	_____
Prof. Dr. Nizami Hasanli	Prof. Dr. Hüsnü Özkan
Co-Supervisor	Supervisor

Examining Committee Members:

Prof. Dr. Bülent Akınoğlu (METU, PHYS) _____

Prof. Dr. Hüsnü Özkan (METU, PHYS) _____

Prof. Dr. Raşit Turan (METU, PHYS) _____

Prof. Dr. Nizami Hasanli (METU, PHYS) _____

Assoc. Prof. Dr. Saffet Nezir (KIRIKKALE UNV., PHYS) _____

I hereby declare that all information in this document has been obtained and presented in accordance with academic rules and ethical conduct. I also declare that as required by these rules and conducts, I have fully cited and referenced all material and results that are not original to this work.

Name, Last name: Nader Ghazanfari

Signature :

ABSTRACT

EFFECTS OF Nb_2O_5 ADDITION ON THE FORMATION AND PROPERTIES OF THE Bi-BASED SUPERCONDUCTORS

Nader Ghazanfari
M.S., Department of Physics
Supervisor: Prof, Dr. Hüsnü Özkan
Co-Supervisor: Prof. Dr. Nizami Hasanli

August 2006, 56 pages

Effects of Nb_2O_5 addition on the formation and properties of the Bi-based superconductors were studied. The superconducting samples were synthesized by two different methods, the solid state reaction (SSR) and ammonium nitrate melt route (ANM) to obtain information about the growth techniques. Ten samples (five with each method) with the chemical compositions of $Bi_{1.6}Pb_{0.4}Sr_2Ca_2Cu_3Nb_xO_y$, with x= 0.00, 0.05, 0.10, 0.20, and 0.30 were prepared.

Phase identification, structural and microstructural analysis were carried out using powder X-ray diffraction method, scanning electron microscopy and energy dispersive X-ray (EDX) analysis. The transition temperature and the critical current measurements were carried out using the electromagnetic measurement system. The critical parameters of the samples were also determined by AC susceptibility and magnetization measurements.

Improvements in the formation of the Bi-2223 phase with Nb addition have been observed by both methods. The ANM method leads mixtures of Bi-2223 and Bi-2212 phases, but with the SSR method pure Bi-2223 phase was obtained.

With small amounts of Nb addition the critical temperature, T_c, remains the same for ANM samples and it increases for the SSR samples. For both series of samples T_c decreases with further increase of Nb content. With Nb addition the critical currents of the ANM sample almost remain the same and those of the SSR samples increases.

Observations based on AC susceptibility measurements showed that Nb addition improve inter-grain coupling. Inductive critical current densities obtained from magnetization measurements agree with the critical currents stated above and show that J_c increase with increase Nb content.

Keywords: High temperature superconductor (HTSC), Bi-based Superconductors, Bi-2223 phase, Critical Temperature, Critical Current, AC susceptibility.

ÖZ

Bi-TABANLI SÜPERİLETKENLERİN OLUŞUMU VE ÖZELLİKLERİNE Nb_2O_5 KATKILAMA ETKİLERİ

Nader Ghazanfari
Yüksek Lisans, Fizik Bölümü
Tez Yöneticisi: Prof. Dr. Hüsnü Özkan
Ortak-Tez Yöneticisi: Prof. Dr. Nizami Hasanli

Ağustos 2006, 56 Sayfa

Bi-tabanlı süperiletkenlerin oluşumuna ve özelliklerine Nb_2O_5 katkılama etkileri çalışıldı. Büyüme teknikleri ile ilgili bilgi edinmek için süperiletkenler katıhal reaksiyonu (SSR) ve amonyum nitrat eriyiği (ANM) olmak üzere iki ayrı yöntemle sentezlendi. Her metotdan 5 adet olmak üzere x = 0.00, 0.05, 0.10, 0.20 ve 0.30 değerleri olan 10 örnek hazırlandı.

X-ışını kırınımı, tarama elektron mikroskop ve enerji soğurma metotları ile faz analizleri, yapısal ve mikro-yapısal analizler yapıldı. Kritik sıcaklık ve kritik akım deneyleri, elektromagnetik ölçüm sistemi ile gerçekleştirildi. Örneklerin kritik parametreleri AC alınganlık ve magnetizasyon yöntemleri ile de belirlendi.

Nb katkılamanın, her iki yöntemde Bi-2223 fazının oluşumuna ve özelliklerine olumlu etki yaptığı gözlendi. ANM yöntemi ile Bi-2212 ve Bi-2223 fazlarının karışık oluştuğu gözlenmiş fakat SSR yöntemi ile saf Bi-2223 fazı elde edilmiştir. Az oranda

Nb katkılama ANM örneklerinin kritik sıcaklıklarını değiştirmemiş fakat SSR örneklerinin kritik sıcaklıklarını artırmıştır. Nb katkılama ile ANM örneklerinin kritik akımları pek değişmemiş fakat SSR örneklerininkiler artmıştır.

AC alınganlık ölçümleri Nb katkılamanın tanecikler arasındaki etkileşimleri küvvetlendıgını göstermiştir. Magnetizasyon ölçümlerinden bulunan kritik akım yoğunlukları yukarıda belirtilen kritik akımlarla nitelik olarak uyumludur.

Anahtar kelimeler: Yüksek Sıcaklıkta Süperiletken, Bi-tabanlı Süperiletkenler, Bi-2223 Fazı, Kritik Sıcaklık, Kritik Akım, AC Alınganlık.

Dedicated to the memory of my father

ACKNOWLEDGEMENTS

I would like to thank Prof. Dr. Hüsnü Özkan for his supervision, guidance, and support during my M.S. studies. I would also like to send my sincere gratefulness to my co-supervisor Prof. Dr. Nizami Hasanli for his efforts through my studies.

I want to present my thanks to Dr. Ahmet Kılıç and Assoc. Prof. Dr. Hüseyin Sözeri for their great help through carrying out this research.

I would like to express my gratitude to my dear friend Selçuk Yerci for motivating me and being by my side and to my friends who were studying from early morning to late hours of day at the department especially Seda Bilgi, Yücel Cengiz Özer, Esen Salçın, and Gülnur Doğan. I would also like to thank all my friends for supporting me morally.

I want to thank all my friends from my hometown who were always by my side and helping me especially Cavit Tebrizli, Yusuf Musevi, Amir Farshchi Tebrizi, Nader Asghar Pour Moghaddam and my great housemate Mohhammed Musevi.

Finally, I am grateful to my mother, brothers, and sisters for their love, care and constant support, especially to my elder brother Firuz for always guiding and encouraging me.

TABLE OF CONTENTS

LIST OF TABLES

TABLES

LIST OF FIGURES

FIGURES

CHAPTER 1

INTRODUCTION

For most materials, under the normal conditions, there is some resistance to the flow of electrical current. It is necessary to apply a voltage to keep the current going, to replace the energy dissipated through the resistance. Superconductivity is the ability of some materials to conduct the electrical current with no resistance below a certain temperature known as the critical temperature (T_c). Superconductivity disappears when the applied current or external magnetic field exceed certain limiting values, which are called critical current (I_c) and critical magnetic field (H_c) respectively.

Superconductivity was discovered in 1911 by Kamerling Onnes [1], a Dutch physicist known for his research studies at extremely low temperatures. He was investigating the electrical properties of different elements at liquid helium temperature when he noticed that the resistivity of mercury dropped dramatically at 4.2 K to zero.

In 1933 Woltter Meissner and Robert Ochsenfeld found that when a superconductor is cooled below its critical temperature, it expels the magnetic flux [2]. During those years it was found that the critical field depends on temperature,

$$H_c(T) = H_0 [1 - (T / T_c)^2] \qquad 1.1$$

where, H_0 is the critical magnetic field at absolute zero.

Superconductors are divided in two types known as Type I and Type II superconductors according to their behavior in a magnetic field. A Type I superconductor completely obeys Meisnner effect but a Type II superconductor have two critical magnetic fields H_{c1} and H_{c2}. Below first critical magnetic field (H_{c1}) it expels magnetic field and above this value magnetic flux penetrate into the material in normal regions surrounded by superconducting ones. The material remains perfect conductor until applied magnetic field exceed second critical magnetic field (H_{c2}). Both H_{c1} and H_{c2} depend on temperature.

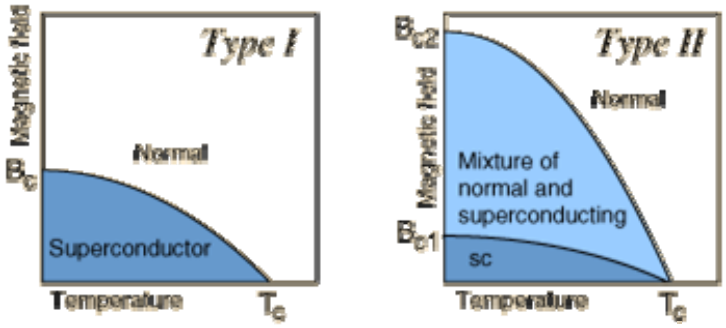

Figure 1.1 Magnetic field versus temperature for Type I and Type II superconductors

In the mixed state, also called vortex state, the magnetic field penetrates into superconductor in quantized units of magnetic flux

$$\Phi = h / 2e = 2.068 \times 10^{-15}\ Tm^2 \qquad 1.2$$

Thus, in the mixed state there are normal regions surrounded by superconducting regions. Vortices in superconductors were discovered by L. V. Shubnikov and coworkers in 1937 [3]. Actually, they discovered the existence of two critical magnetic fields for Type II superconductors. During electrical conduction the Lorentz force may cause vortices to move. Motion of vortices may cause energy dissipation and destroy superconductivity.

In 1950, H. Frohlich proposed that atomic vibrations play an important role in superconductivity. Following this proposal, the isotope effect was found in the same

year by E. Maxwell and C. A. Reynolds [4, 5]. They found that the critical temperature of superconductors depends on isotope mass. The isotope mass is a characteristic of the crystal lattice and can effect its properties. Subsequent developments indicate that superconductivity is due to the interaction of the electron with the lattice. The theory of superconductivity was developed soon after the discovery of this effect. In 1957 John Bardeen, Leon Cooper, and Robert Schrieffer developed the theory of superconductivity, called the BCS theory [6]. A key conceptual element in this theory is the pairing of electrons as Cooper pairs through interaction with the crystal lattice.

After the discovery of the superconductivity, efforts were devoted to increase their transition temperatures. For more than half a century researchers was focusing on Nb-based superconductors (Nb has the highest transition temperature among the superconducting elements) but breakthrough to high-temperature superconductors could be achieved on completely different compounds having copper, oxygen and other elements. In 1986 a new high T_c superconductor was discovered in a compound of lanthanum, barium, copper, and oxygen by Georg Bednorz and Alex Muller [7]. The oxide superconductor, $La_{2-x}Ba_xCuO_4$, had a critical temperature of 35K. In 1987 C.K. Wu and his associated M.K. Wu [8] could raise the critical temperature to 52.5 by applying pressure to the sample. Then the same group came with a clever idea of creating internal pressure by atomic substitution. The resulting yttrium-barium-copper oxide was a high temperature superconducting material with T_c greater than 90 K. The identification of the $Y_1Ba_2Cu_3O_7$ (YBCO or 1-2-3) revealed that it has completely different crystal structure than the La-based superconductor.

The efforts to find additional high temperature superconductors lead to the discovery of bismuth-strontium-calcium-copper oxide (BSCCO). In 1987 Raveau [9] found superconducting phase in the Bi-Sr-Cu-O system with T_c around 80 K. Soon after that, Maeda et al. [10] discovered superconducting phase in the Bi-Sr-Ca-Cu-O with T_c around 110 K. These were followed by the discovery of thallium barium calcium copper oxide, with T_c= 125 K [11]. Almost five years later the mercury compounds boosted the T_c= 135 K [12].

The high-temperature superconductors are ceramic materials having copper- oxygen planes. Such planes are believed to play important role in the mechanism of superconductivity. Transition temperatures of the ceramic superconductors depend on the charge carrier concentration in the Cu-O planes. High temperature superconductors are Type II superconductors having extremely high critical magnetic fields, H_{c2}. Their properties are very anisotropic; properties are quite different in different crystalline directions. The coherence length of these superconductors is very short.

The high-temperature superconductors have two major drawbacks: they are brittle, and their critical current density is very low. They are not suitable for making wires and tapes.

Yttrium-based superconductors are very sensitive to humidity, Tl and Hg-based superconductors are not suitable for safe handling and for the industrial applications despite their high T_c. The Bi-based superconductors have better properties compared with other high temperature superconductors. Different phases of the Bi-based superconductors can be formed having different composition, structure and properties.

There are several ways of enhancing preparation methods and superconducting properties of high temperature superconductors: Charged particle irradiation, substitution of different atoms, and alteration of microstructure during processing. Since the discovery of high temperature superconductors many substitution experiments have been carried out to stabilize formation of BSCCO. During processing different phases of the Bi-based superconductors may be formed. It is quit difficult to obtain pure form of the desired phase. Different elements have been doped to improve the superconducting properties and to obtain the isolated phases. Lead is one of such doping element shown to improve the stability of the different phases of the Bi-based superconductors.

Nb is another element that may have positive effect in this regard. There are limited data in the literature about the effect of Nb on the properties of the Bi-based

superconductors. In these studies Nb were stated to increase J_c and promote the formation and stability of the high T_c phase (Bi-2223). On the other hand the microstructure and the properties of the superconductors depend on growth method. Essentially there are two methods, solid state and wet method using ammonium nitrate melt. The solid state method usually lead larger grains but ammonium nitrate method result with more homogenous mixing of oxides and lead to widespread growth of small grains.

We aim to study the effect of Nb on the Bi-based superconductors grown by both solid state reaction and ammonium nitrate melt method. This way we will explore not only the effect of Nb doping of different concentrations but also investigate comparatively the effect on the samples grown by different methods having different microstructural features.

Previous studies, about the effects of Nb substitution on properties of BSCCO [13-17] pointed out that Nb improves phase stability of the different phases [13, 14] and improves the critical current density in this system [15]. Mishra et al. [16] reported that T_c decreases by increasing Nb concentration in both Bi and Cu-sites. Some other studies have reported that Nb remains neutral in the superconducting lattice and have minimal effects on the properties [17].

In this thesis firstly the fundamental concepts, crystal structure and the properties of the copper oxide superconductors are presented. Then the formation mechanism and preparation methods of the ceramic superconductors are explained. The effects of doping on high temperature superconductors are reviewed. Preparation and characterization of Nb_2O_5 added bulk ceramic $Bi_{1.6}Pb_{0.4}Sr_2Ca_2Cu_3O_{10}$ (Bi-2223) superconductors are presented. After that, the effects of Nb_2O_5 addition on formation and properties of the Bi-based high temperature superconductors prepared by two different methods are discussed. Finally the conclusions of this study are presented.

CHAPTER 2

HIGH TEMPERATURE CERAMIC SUPERCONDUCTORS

2.1 Introduction

Before the discovery of the high temperature superconductivity, the highest transition temperature obtained for Nb_3Ge as 23.2 K. Oxides are normally insulators but they show strong electron-phonon interactions. This property, under certain conditions, leads them to become good superconductors.

2.2 Common Properties of the Copper Oxide Superconductors

All cuprates have some features in common. The most important feature of the copper oxide superconductors is to have layered crystal structure consisting of one or more Cu-O planes. The Cu-O planes are considered to conduct supercurrent. The transition temperatures of these superconductors are closely correlated with the number of Cu-O layers in the unit cell, and the charge carrier concentration in the layers. The Cu-O layers are separated by arrays of other atoms. The intervening layers can be divided into two categories: structural layers and charge reservoirs. The structural layers, like Y layer in YBCO, play a minor role in the variation of the T_c, but the charge reservoir layers have a large impact on T_c. The distance between CuO_2 planes and the charge reservoir layers, which provide the charge carriers into Cu-O planes is also important. The crystal structures of the HTSCs are all anisotropic. The anisotropy of the crystal structure manifests itself in the electrical conduction, with high-conductivity in the Cu-O planes. The conduction

perpendicular to the Cu-O layers is less by about two to four orders of magnitude depending on the specific compound and the quality of the crystal used.

Another important feature is that the Cu-O planes have to be doped to improve electrical conduction. By doping electrons are removed from the planes, leaving behind vacancies (holes). When enough holes are created the Cu-O layers behave as metallic, to become superconducting. Thus the transition temperature strongly depends on the carrier concentration in the Cu-O planes. There are two ways to increase the number of charge carriers in cuprates: to substitute metallic atoms in charge reservoirs by higher-valance atoms, and to change the oxygen concentration. In the most superconducting cuprates, T_c has a maximum value for an optimum hole concentration. At a fixed doping level, N_l, T_c first increases by increasing the number of CuO_2 planes, reaching the maximum at $N_l = 3$, and then T_c decreases.

2.3 Superconducting State

The cuprates display same properties that are similar to those of conventional superconductors. The experiments have demonstrated that their superconducting state is made up of paired carriers. The investigations have shown that copper oxide superconductors also exhibit an energy gap in the superconducting state as conventional ones do. As conventional superconductors a jump in the heat capacity is observed at $T=T_c$, which indicates that the origin of the phase transition is similar. On the other hand there are some differences between these two types. For example, superconducting coherence length is extremely short (10^{-7} cm) for copper oxide superconductors compared with conventional ones, which have the coherence length of approximately 10^{-4} cm. The fraction of the carriers directly involved in the pairing is very large in high temperature superconductors. There are some differences in the behavior of the elastic constants above and below the transition temperature.

2.4 Crystal Structure of High Temperature Superconductors

Structural features play important role for superconductivity in HTSCs. Therefore, it is useful to consider structural parameters that affect transition temperature. It is

stated that superconductivity in cuprates occurs in CuO_2 planes. Thus the structural parameters and geometry of theses planes affect T_c. For example, in the case of mercury compound the influence of Cu-O length on T_c is well demonstrated and the highest T_c corresponds to the shortest Cu-O bond.

All ceramic superconductors are composed of similar building blocks, which can be closely related to the classic perovskite ABO_3 Structure. In the following sections the crystal structure and superconducting properties of the yttrium based and bismuth based superconductors are presented.

2.4.1 $YBa_2Cu_3O_{7-\delta}$

$YBa_2Cu_3O_{7-\delta}$ was the first high temperature superconductors to have T_c above the liquid nitrogen temperature (77 K). It has only four element, least among HTSCs with a T_c higher than 77 K. Structurally, oxygen deficient $YBa_2Cu_3O_6$ (δ= 1) and fully oxygenated compositions $YBa_2Cu_3O_7$ (δ= 0) can be formed. This compound for $0.5 < \delta < 1$ is orthorhombic, superconducting, and for $0 < \delta < 0.5$ tetragonal, nonmetallic. The variation in oxygen concentration is easily achieved by heating under different oxygen partial pressure. The high-T_c phase of $YBa_2Cu_3O_7$ have an orthorhombic structure with element ratio 1:2:3:7 and the lattice parameters of a= 3.82 Å, b= 3.89 Å and c= 11.68 Å. Yttrium can be replaced by the rare earth elements without affecting the structure significantly and with negligible effect on the critical temperature. The $YBa_2Cu_3O_7$ is often called as YBCO or 1-2-3 compound because of the ratios of its constituents.

The crystal structure of nonmetallic $YBa_2Cu_3O_6$ and superconducting $YBa_2Cu_3O_7$ are shown in figure 2.1. The Cu-O planes or layers and Cu-O chains can be seen in the figure. The chains consist of Cu and O atoms along the b axis, at (0,0,0) and (0,1/2,0), respectively and each O ion is shared by two Cu atoms. The layers consist of Cu sites at $(0,0,z_{Cu})$ neighbored by O sites at $(1/2,0,z_O)$ and $(0,1/2,z_O)$. The Y site is at (1/2,1/2,1/2) and the Ba sites are at $(1/2,1/2,z_{Ba})$. The structural parameters depend on the stoichiometry and history of the sample.

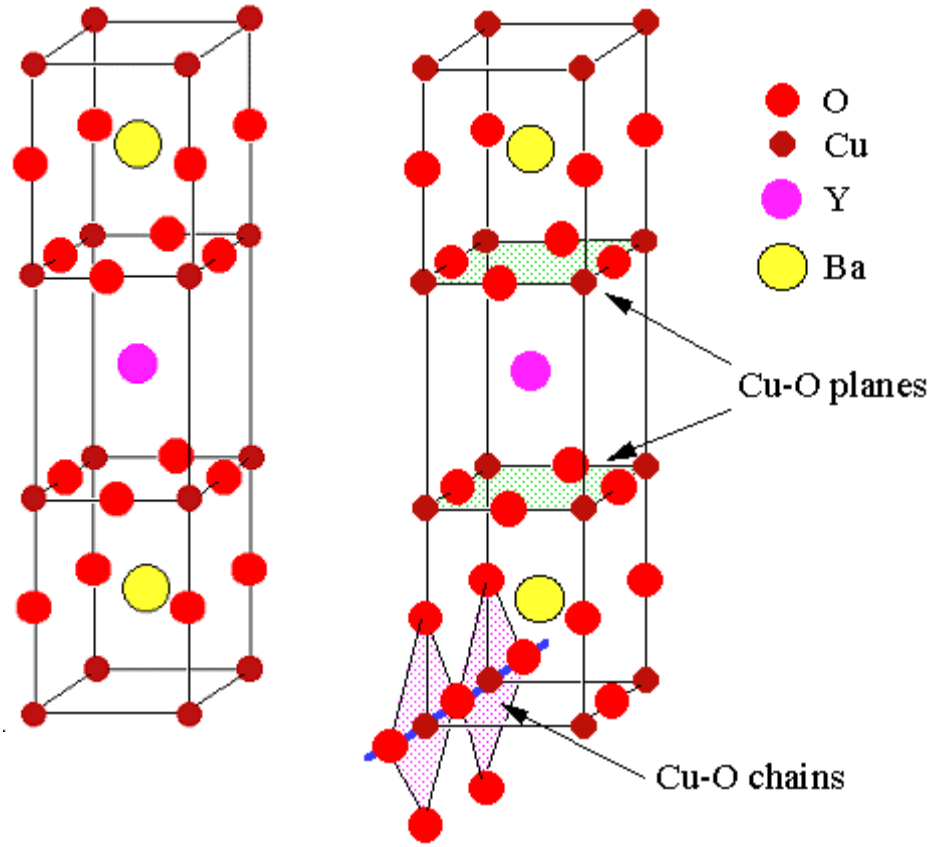

Figure 2.1 Crystal structures of the Y-Ba-Cu-O system

Critical temperature of YBCO is about 90 K, and very sensitive to the oxygen content. The upper critical magnetic field of YBCO is stated to be 14 T at liquid nitrogen temperature and at least 60 T at 77 K.

2.4.2 Bi-based Ceramic Superconductors

The general formula for Bi-based HTSCs can be stated as $Bi_2Sr_2Ca_{n-1}Cu_nO_{2n+4}$. Hence, n can take (n=1,2,3) values for the different number of Cu-O planes perpendicular to the c-axis. This system is usually called as BSCCO and the phases are usually stated by the atomic ratio of the constituent elements of Bi:Sr:Ca:Cu as Bi-2201, Bi-2212, Bi-2223 for n= 1,2,3 respectively. The crystal structures of three phases of the Bi-based superconductors are illustrated in figure 2.2.

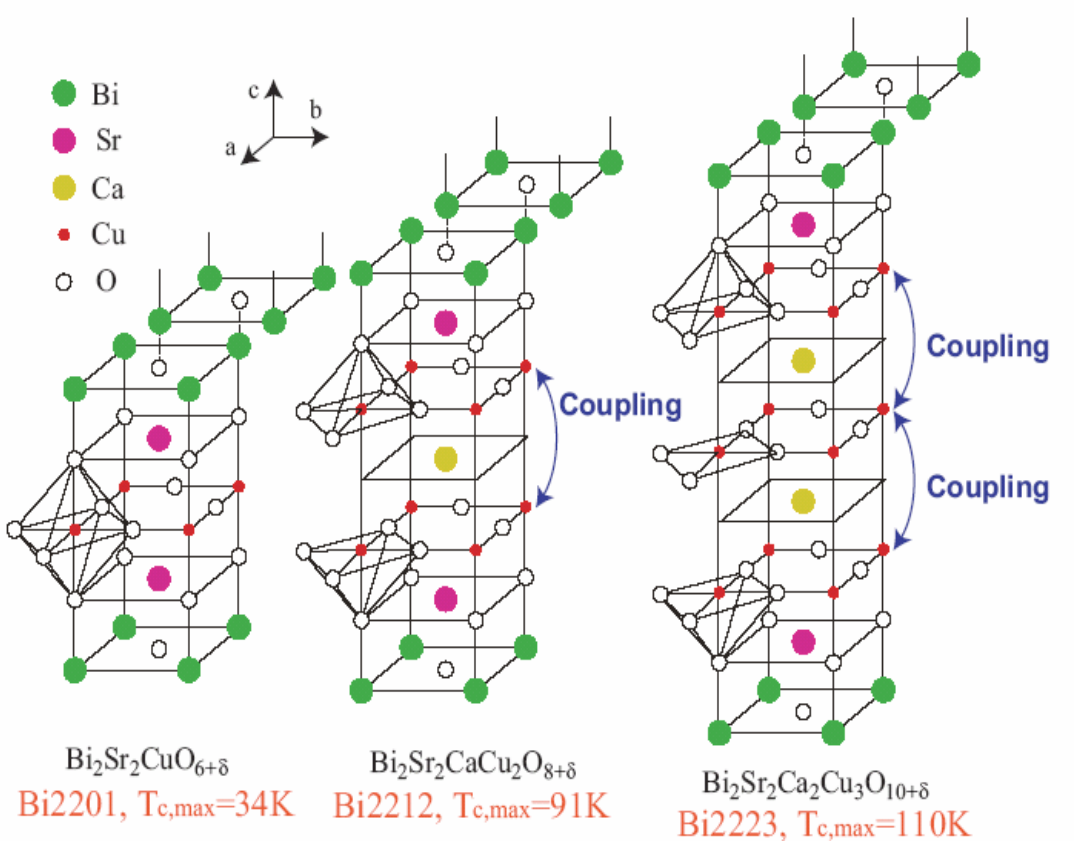

Figure 2.2 The crystal structure of Bi-based high temperature superconductors

For n= 1 phase, the structure contains two Sr_2O_2 layers that are separated by Bi_2O_2 double layers, and CuO_2 single layer and no Ca layer. The n= 2 phase contains 14 layers per unit cell. The Cu-O sheets in Bi-2201 are replaced by CuO_2-Ca-CuO_2 sandwiches in Bi-2212 with a layer sequence Bi_2O_2-Sr_2O_2-CuO_2-Ca-CuO_2-Sr_2O_2-Bi_2O_2. The structure of Bi-2223 is similar to that of the Bi-2212 phase, but additional CuO_2 and Ca layers are inserted within the CuO_2-Ca-CuO_2 sandwich of Bi-2212, yielding a CuO_2-Ca-CuO_2-Ca-CuO_2 sandwich. The unit cell consists of 18 layers with c= 37.1 Å.

The transition temperatures of the different phases are related to the number of the Cu-O layers per unit cell. T_c increases with increasing the number of planes. Critical temperatures of Bi-2201, Bi-2212, and Bi-2223 are 4, 91, and 110 K, respectively. All three phases have tetragonal structure. They have approximately the same lattice

parameters along the a-axis, but normally different lattice parameters along c-axis. For Bi-2201 phase c= 24.6 Å, for Bi-2212 phase it is c= 30.6 Å, and for Bi-2223 phase c= 30.6 Å.

The structural anisotropy and the existence of the Cu-O layers greatly affect the physical properties of these compounds. The single crystals of the anisotropic compounds Bi-2212 and Bi-2223 may be cleaved along the ab-plane without damaging the basic structure of the compound. The BSCCO grains may be aligned better than the grains other ceramic superconductors. This is an advantage to produce high quality tapes and wires. Thus more investments and efforts were devoted on this ceramic superconductor. Similar structures of $Bi_2Sr_2Ca_{n-1}Cu_nO_{2n+4}$ can be formed for the Tl-based superconductors, as $Tl_2Ba_2CuO_6$, $Tl_2Ba_2CaCu_2O_8$, and $Tl_2Ba_2Ca_2Cu_3O_{10}$. These are regarded as isomorphous with Bi-2201, Bi-2212, and Bi-2223, respectively.

2.5 Preparation of High Temperature Ceramic Superconductors

The high temperature superconducting phases have several elements in different proportions. The word phase is used to define any homogeneous and physically distinct part of a material system which is separated from other parts by well-defined boundaries. During processing usually different phases could be formed. The important task is to prepare the desired phase in pure form. For the case of the BSCCO under normal preparation conditions, usually the mixture of Bi-2212 and Bi-2223 phases may be obtained. Then several routs are applied to increase the Bi-2223 phase. The preparation of the Bi-2223 phase is important, as its T_c is relatively high.

High-temperature superconductors belong to a family of materials known as ceramics. Ceramics are products made from inorganic and nonmetallic elements. Manufacturing of ceramics usually consist of three main steps. Firstly, ceramic powder with desired particle size is prepared. Then the powder is shaped and densified by applying pressure. Finally the ceramic is sintered at high temperature to obtain a coherent polycrystalline solid.

Many synthesis routs have been developed in order to produce HTSCs. In all theses methods appropriate amount of oxides are mixed and calcined. The different routs of powder preparation may be classified as a solid state process and liquid phase process. In the solid state process, metal oxide and carbonate powders are mixed, and calcined. In the liquid phase process the oxides are mixed with appropriate liquid material, which is eliminated by evaporation. In the following sections the solid state reaction and the ammonium nitrate melt methods are explained.

2.5.1 Solid State Reaction Method

The solid state reaction method is a general method to produce HTSCs. The process consists of selection of raw materials, weighing, mixing, calcining and pulverizing steps. Figure 2.3 illustrates the flowchart for the solid state process to form powder of the Bi(Pb)-Sr-Ca-Cu-O system.

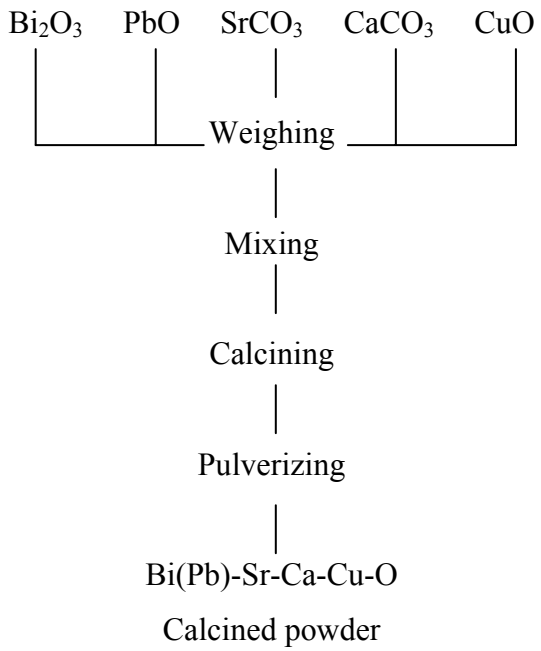

Figure 2.3 Flowchart for solid-state process calcined powder.

The following characteristics of the raw material powder are desired: A primary particle size is fine and shape is spherical. The characteristics of the superconductor

depend strongly on the shape and size of the starting raw materials. The superconductivity of the product is significantly dependent on the molar ration of the oxides used. Particular attention should be given to mix correct amounts of the powders. The raw materials are mixed by means of a ball-mill. Homogenous mixture of the oxides should be obtained and the particle size should be reduced, to achive high solid state calcination. The mixed powder is heated for 10-50 h at the 800-850 °C to result the synthesized calcined powder. Carbon contaminants degrade the superconducting characteristics of the product. Sufficiently long or repeated calcinations are applied to reduce the residual carbon. Calcination under oxygen flow and/or vocume (10^{-1}–10^{-3}) Torr are effective to obtain calcined powder of high purity and high reactivity. In the synthesis of the calcined powder by solid state reaction, the resultant powder becomes grained or aggregated. In order to sinter the specimen sufficiently it is necessary to pulverize the grain by means of a ball-mill.

2.5.2 Ammonium Nitrate Melt Method

The ammonium nitrate melt process consists of dissolving the compounds containing the elements in a solvent. The solvent subsequently evaporate and the the superconductor are formed by usual heat treatments. One important characteristics of this method is to form homogeneous mixture of powders before the calcination and sintering reaction. Ammonium nitrate ($NH_4.NO_3$) is used to solve the metal oxides. Appropriate amount of the oxides are mixed in certain amount of ammonium nitrate solution and heated up to certain temperature to obtain the desired homogeneous powder. During the heating the solution is mixed to maintain the homogeneity. In this step ammonium nitrate decomposes into ammonium, water and oxygen.

$$NH_4NO_3\text{------}NH_3+H_2O+\text{Oxygen}+\text{heat} \qquad 2.1$$

The decomposition process is exothermic and liberates oxygen. The heat out put during decomposition of NH_4NO_3 helps for the calcination of the metal nitrates. Some of the released oxygen atoms enter the reaction and help sinter samples with higher oxygen stoichiometry.

CHAPTER 3

EFFECTS OF DOPING ON PROPERTIES OF THE HIGH TEMPERATURE SUPERCONDUCTORS

3.1 Introduction

The copper oxide superconductors are perovskites which are usually insulators. HTSCs are usually doped to improve their superconducting properties.

The existence of an energy gap and the electronic density of states in Fermi level are the essential characteristics of any superconductor. It is possible to increase the number of the electrons or holes in the superconductor by doping. The transition temperature depends on the density of carriers. In other words, T_c may be influenced by doping the superconductor with atoms of a different valence, to provide extra electrons or holes (absence of electrons).

The charge carrier concentration in HTSCs is low compared with low temperature superconductors. Doping may be an effective choice to increase the number of charge carriers. In the following sections the effects of doping on the properties of HTSCs are discussed.

3.1.1 Structural Defects and Vortices

In Type II superconductors magnetic vortices penetrate into the superconductor when the external field H exceeds the value H_{c1}. When an electric current J passes through the sample, Lorentz force acts to the vortices

$$\mathbf{F} = \mathbf{J} \times \mathbf{B} \qquad 3.1$$

The force may displace the vortices that in turn may create resistance, which cause energy dissipation and destroy superconductivity. There must be some mechanism to prevent the Lorentz force from moving the vortices. Such a mechanism may create pinning force to pin the vortices at fixed positions.

Under appropriate condition the non-superconducting regions in the superconductor may act as pinning sites for the vortices. These regions may be microstructural inhomogeneities and structural defects. The strength of pinning forces depends on the nature and types of defects. The defects having dimension close to the coherence length of the superconductor may act as pinning centers for the magnetic flux lines. This way it is possible to enhance the superconducting properties (higher critical currents, better performance under high magnetic field, etc.). Defects having dimension greater than the coherence length may be detrimental to the superconducting properties. The defects in the superconductors may be created by doping with different atoms.

3.1.2 Cu-O layers and Electrical Conduction

In HTSCs, the supercurrent flows in a sandwich formed by CuO_2 planes, which are separated by a single atom. These planes are called the conduction layers. Ideally, the oxygen atoms in these layers are left undisturbed. Indeed, if the CuO_2 planes are seriously disrupted, superconductivity is destroyed. The remainder of the unit cell serves as charge reservoir. The role of a defect (or substituted atom) in any HTSC is to alter carrier concentration (electrons or holes) in the CuO_2 planes. In all the HTSCs, the CuO_2 planes also determine the size of the unit cell. The mercury

compounds have the highest T_c values due to having perfectly flat CuO_2 planes. Thus, superconductivity in all the HTSCs depends on the details of the layer structure, and that depends on the distortions produced by lattice defects or by various dopant atoms.

3.1.3 Oxygen content and Superconductivity

The role of oxygen in high temperature superconductors is very important. In chemistry, it is not guaranteed that the oxygen will appear in exact stoichiometric proportion. Let's see how the electron vacancy affects the charge balance in a crystal. Normally an oxygen atom takes two electrons from other atoms. As oxygen atom is missing two electrons are freed in the lattice. For example; in $YBa_2Cu_3O_{7-\delta}$ the δ refers to the electron vacancies from the normal number 7 which corresponds to a crystal lattice without oxygen vacancies. Superconductivity disappears when the value of δ exceeds 0.5. There is a fairly narrow range of oxygen deficiencies required to achieve superconductivity in the copper oxides.

The first and most important effect of oxygen deficiencies is changing the number of free carriers in the lattice. The number of free carriers influences the density of states N_0 at the Fermi level, a key parameter of superconductors. As it is discussed before, the critical temperature of superconductors strongly depends on the density of states at Fermi level, and small changes in N_0 caused by oxygen vacancies can have substantial changes in T_c.

There are several different ways of causing charge transfer in BSCCO: missing metal atoms, extra metal atoms, missing oxygen, extra oxygen, and so forth.

Finally, it should be noted that excess oxygen increases the number of sites for electrons to reside. This creates holes in the crystal; thus, extra oxygen atoms act as dopant. The compound La_2CuO_4 is normally an insulator, but when oxygen concentration is increased in La_2CuO_{4+x} it becomes a superconductor.

3.1.4 Valance Electrons and Charge Carriers

For a material to be called a metal, there must be empty states in the energy bands for electrons or holes to move freely. The way for an insuletor to bahave as a metal is to add or subtract electrons. The way to do this is by doping.

The experiment of Bednorz and Muller involved doping the parent compound La_2CuO_4 with barium, to see how its properties would change. The result was a pleasant surprise. The compound La_2CuO_4 is an insulator, but when some strontium (valence = +2) is substituted for lanthanum (valance= +3), by this charges depart from the copper oxide planes, leaving behind holes that carry the supercurrent. The substituted compound becomes a metal. In other words the unoccupied states are left in a band, to give freedom of movement to the electrons. The result is the superconducting compound $La_{2-x}Sr_xCuO_4$ with T_c= 38 K.

3.2 Effects of doping on Superconducting Properties of BSCCO

The goal of most substitutions is to change the number of carriers by doping the various layers of the unit cell. Comparatively few substitution experiments have been done for copper atoms and more substitution studies have been carried out for the sites occupied by the other atoms. The Cu-O planes carry supercurrent. The other planes act as charge reservoirs for Cu-O planes. Logically the most attention and experimentation should go to modify these sites. For BSCCO, each investigator arranges a doping strategy according to his aims to obtain the desired properties. The most known substitution in BSCCO series is to replace bismuth by lead. This substitution has minor effects on the superconducting properties, but has major effects on phase equilibrium of the compound. For example; Pb substitution for Bi not only stabilizes the high-T_c phase Bi-2223 but also increase its volume fraction. This means that producing (Bi,Pb)-2223 is much easer than producing of Bi-2223.

The range of possible substitutions in high temperature superconductors is very enormous. The motivation of the doping strategy is to manipulate the carrier concentration without drastically altering the basic structure. The goal of such a

research studies is to establish an experimental foundation on which a theory can be built to explain the mechanism of HTSCs.

CHAPTER 4

EFFECTS OF Nb_2O_5 ADDITION ON THE FORMATION AND PROPERTIES OF THE Bi-BASED SUPERCONDUCTORS

4.1 Introduction

There are several ways of enhancing preparation methods and properties of high temperature superconductors. Two of the mostly used ways are ion irradiation and atom substitutions. Over the years many substitution experiments have been carried out to improve the stability and formation of BSCCO.

Several studies have been carried out about the effects of Nb on the BSCCO system [13-17]. In some of them it was reported that Nb has a similar effect as Pb; it enhances the formation and stability of Bi-2223 phase [13,14]. In some studies it was mentioned that Nb improves the critical current density of BSCCO [15]. However, there are some controversial reports on its effects for the Bi-2223 phase. Mishra et al. [16] reported that T_c decreases by increasing Nb concentration in both Bi and Cu-sites. On the other hand, in some studies it has been stated that Nb remains neutral to superconductivity [17].

In this chapter, the experimental procedure for the synthesis and characterization of the Pure and Nb added BSCCO samples are explained, and the related analysis are presented. Sample preparation techniques are explained. Then the measurements, the collected data, and the results are discussed. The data Obtained and the

measurements are compared with the related experiments and studies in the literature. Finally the conclusion of this research is presented.

4.2 Experimental Details

4.2.1 Sample Preparation

Two series of samples with the chemical composition of $Bi_{1.6}Pb_{0.4}Sr_2Ca_2Cu_3Nb_xO_y$, with x=0.00, 0.05, 0.10, 0.20 and 0.30 were prepared by two different methods, the solid state reaction and ammonium nitrate melt method. The aim is to study the effect of Nb_2O_5 on the formation and superconducting properties of Bi-2223 phase. The samples were prepared according to the chemical reaction

$$0.8Bi_2O_3+0.4PbO+2SrO+2CaCO_3+ 3CuO+(x/2)Nb_2O_5 \longrightarrow Bi_{1.6}Pb_{0.4}Sr_2Ca_2Cu_3Nb_xO_y+Gases \quad 4.1$$

where, x= 0.00, 0.05, 0.10, 0.20, and 0.30.

The amount of each oxide or carbonate powder was determined by the equation

$$M(gram) = \frac{N(gram).A(a.u.)}{T(a.u.)} \quad 4.2$$

where N is the amount of the sample in grams, A is the atomic weight of the oxide or carbonate used and T is the total atomic weight of the oxides and carbonates. After determining the proper amounts (M's) for each sample, powders of ten samples were prepared, five samples for SSR and five for ANM method.

For the case of SSR method N= 1.2 gram was prepared for each sample. The amounts of powders are given in Table 4.1. The powders were mixed and grounded by means of an agate mortar to reduce particle size and increase homogeneity. The mixed powders were calcined for 24 hours at 800 °C using a Protherm furnace. After first calcination the carbon is eliminated and a black powder is obtained. The black

powders were regrained and pressed into pellets by applying 5 MPa pressure. The pellets were calcinated for the second time at 850 °C for 75 hours. After this calcination samples were slowly cooled to room temperature and then regrained and palletized. The last calcination was applied at 840 °C for 96 hours and the samples were cooled slowly to room temperature.

For the ANM route appropriate amounts of powders were mixed in AN solution which was kept at 170 °C. Then the solutions were heated to 250 °C to evaporate ammonium nitrate and to get BSCCO precursors. The precursors were then pressed into pellets under 250 MPa pressure. The pellets were calcined at 850 °C for 75 hours as the SSR samples. The samples were regrained, palletized and calcinated again at 840°C for 96 hours. During the sintering the same heat treatments were applied for both SSR and ANM methods.

Table 4.1 The amounts of the oxides used for Nb-free and Nb added SSR samples

COMPOUND	A (A.U.)	M (GRAM) NB FREE SAMPLES	M (GRAM) NB ADDED SAMPLES
Bi_2O_3	465.96	0.5750	0.4514
PbO	223.20	0.1377	0.1081
SrO	103.62	0.3197	0.2425
$CaCO_3$	100.09	0.3088	0.2891
CuO	79.55	0.3681	0.2511
Nb_2O_5	265.82	-	0.0080, 0.0161, 0.0322, and 0.0483 respectively for x= 0.05, 0.10, 0.20, and 0.30

4.2.2 Details of the Measurements

The powder X-ray diffraction patterns were obtained to study the formation of the high and low T_c phases and the structures of the samples. Rigaku X-ray diffractometer with CuKα radiation was used. All measurements were taken between 2θ=3.5° up to 2θ=60° by a sampling range of 0.02° and scan speed of 2 degree per minute.

The structural and microstructural properties of the samples were investigated using scanning electron microscope (JEOL 6335F Field emission Gun) and energy dispersive X-ray (EDX) analysis.

Transition temperature measurements and I-V characterizations were carried out by standard four-probe method utilizing a digital nanovoltmeter and a constant current source. The samples were cooled using a liquid nitrogen cryostat with N_2 as heat exchanger. The measurements were taken by heating the samples from 80 K up to 150 K. The transition temperatures and critical currents were determined. T_c for each sample was determined by applying 20 mA constant current.

AC Susceptibility measurements were performed using a Lake Shore 7130 AC susceptometer with a closed-cycle refrigerator at low temperatures down to 15 K. The samples kept in helium exchange gas with a controllable temperature resolution of 10 mK. They were moved from the centre of one secondary to the other to eliminate unwanted signals and to maximize the main signal. The phase angle was adjusted to separate real and imaginary parts of the susceptibility. The measurements were taken from 45 K up to 110 K.

Inductive critical current densities of the samples were also calculated using the Bean Model [18] from the magnetization measurements which were carried out using a SQUID magnetometer from Quantum Design. This part of measurements was carried out at TUBITAK-UME, National Metrology Institute, Gebze, Kocaeli.

4.3 Results and Discussions

4.3.1 XRD Measurements

The XRD patterns of the SSR and ANM samples are shown in Figure 4.1 and Figure 4.2, respectively. The effects of Nb_2O_5 addition on formation of the high and low-T_c phases in the Bi-based superconductors were investigated by qualitative and quantitative analysis using the Rigaku miniflex software. The XRD studies show that both Bi-2223 and Bi-2212 phases coexist in most of the samples. The volume fraction of the Bi-2223 and Bi-2212 phases in each sample were determined and presented in Table 4.2. For the ANM samples with x= 0.20 and x= 0.30 there are some other phases, which have been taken in volume fraction calculation of samples.

Table 4.2 Volume fraction of high-T_c and low-T_c phases for SSR and ANM samples

	ANM		SSR	
Nb concentration	Bi-2223 phase %	Bi-2212 phase %	Bi-2223 Phase %	Bi-2212 Phase %
x= 0.00	38	62	35	65
x= 0.05	40	60	48	52
x= 0.10	55	45	100	0
x= 0.20	50	45	95	5
x= 0.30	45	10	85	15

The XRD patterns for SSR and ANM samples are plotted together in Figure 4.3. The volume fractions of Bi-2223 phase in the ANM samples do not differ much with increase of the Nb content. However, as the Nb concentration increases Bi-2223 phase enhances sharply in the samples sintered via SSR method. For the SSR sample with x= 0.10, there is only Bi-2223 phase seen in the XRD pattern and Bi-2212 phase disappears. This means that, almost pure Bi-2223 has been sintered, and

suggesting x= 0.10 to be the optimal Nb concentration to obtain the pure Bi-2223 phase. The low-T_c phase reappears with increase of Nb content for x= 0.20 and x= 0.30, but the amount of Bi-2212 phase is much less than that in the Nb-free sample. These observations and the increase of volume fraction of the Bi-2223 phase suggest that Nb addition may have similar effect and play the same role as the Pb substitution in Bi-based superconductors. Similar enhancement in volume fractin of the high-T_c phase has been observed in some previous studies [13,14], specially Li et al. [14] reports the role of Nb substitution is quit similar to that of Pb substitution.

4.3.2 Energy Dispersive X-ray (EDX) Analyses

Chemical compositions of the samples were determined by energy dispersive X-ray (EDX) analyses. The data obtained from EDX are given in the Appendix A. The chemical compositions of the samples are presented in Table 4.3. The results show that Nb is incorporated in all added samples and the concentrations of Nb in ANM samples are more than that in the SSR samples. This is an expected result as ANM route exhibit better homogeneity for powder mixing. The other important feature is the noticeable differences in the oxygen contents for Nb added samples compared with Nb free samples. The SSR sample with x= 0.10 Nb exhibits the highest oxygen content. This increase in oxygen content may be due to adding Nb_2O_5, which release additional oxygen during synthesis. The extra oxygen released during the reaction of the Nb_2O_5 may increase the oxygen content and improve the superconducting properties of added samples.

Table 4.3 Chemical compositions of the SSR and ANM samples

Nb	ANM route	SSR route
0,00	$Bi_{1.7}Pb_{0.2}Sr_2Ca_{1.94}Cu_{3.98}O_{9.54}$	$Bi_{1.36}Pb_{0.28}Sr_2Ca_{1.67}Cu_{2.92}O_{8.36}$
0,05	$Bi_{1.67}Pb_{0.38}Nb_{0.13}Sr_2Ca_{1.77}Cu_{3.11}O_{11.31}$	$Bi_{1.73}Pb_{0.29}Nb_{0.1}Sr_2Ca_{1.8}Cu_{3.35}O_{9.82}$
0,10	$Bi_{1.69}Pb_{0.34}Nb_{0.2}Sr_2Ca_{1.83}Cu_{3.24}O_{11.41}$	$Bi_{1.73}Pb_{0.3}Nb_{0.15}Sr_2Ca_{2.11}Cu_{3.28}O_{13.09}$
0,20	$Bi_{1.74}Pb_{0.33}Nb_{0.24}Sr_2Ca_{1.75}Cu_{3.22}O_{10.53}$	$Bi_{1.78}Pb_{0.26}Nb_{0.24}Sr_2Ca_{1.99}Cu_{4.6}O_{11.39}$
0,30	$Bi_{1.98}Pb_{0.29}Nb_{0.4}Sr_2Ca_{1.84}Cu_{2.82}O_{11.3}$	$Bi_{1.57}Pb_{0.27}Nb_{0.25}Sr_2Ca_{1.74}Cu_{3.5}O_{10.95}$

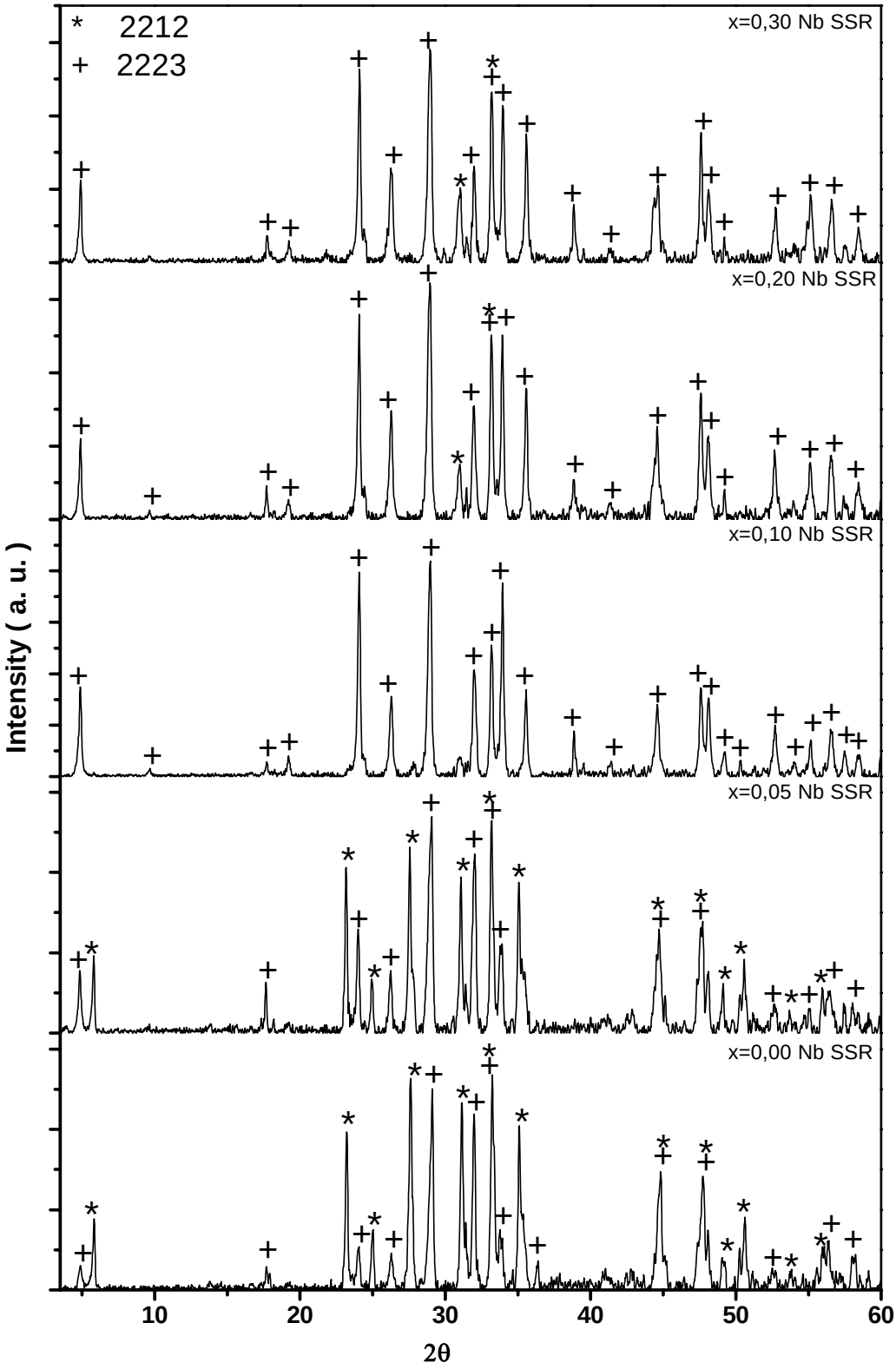

Figure 4.1 XRD patterns of samples prepared with SSR method

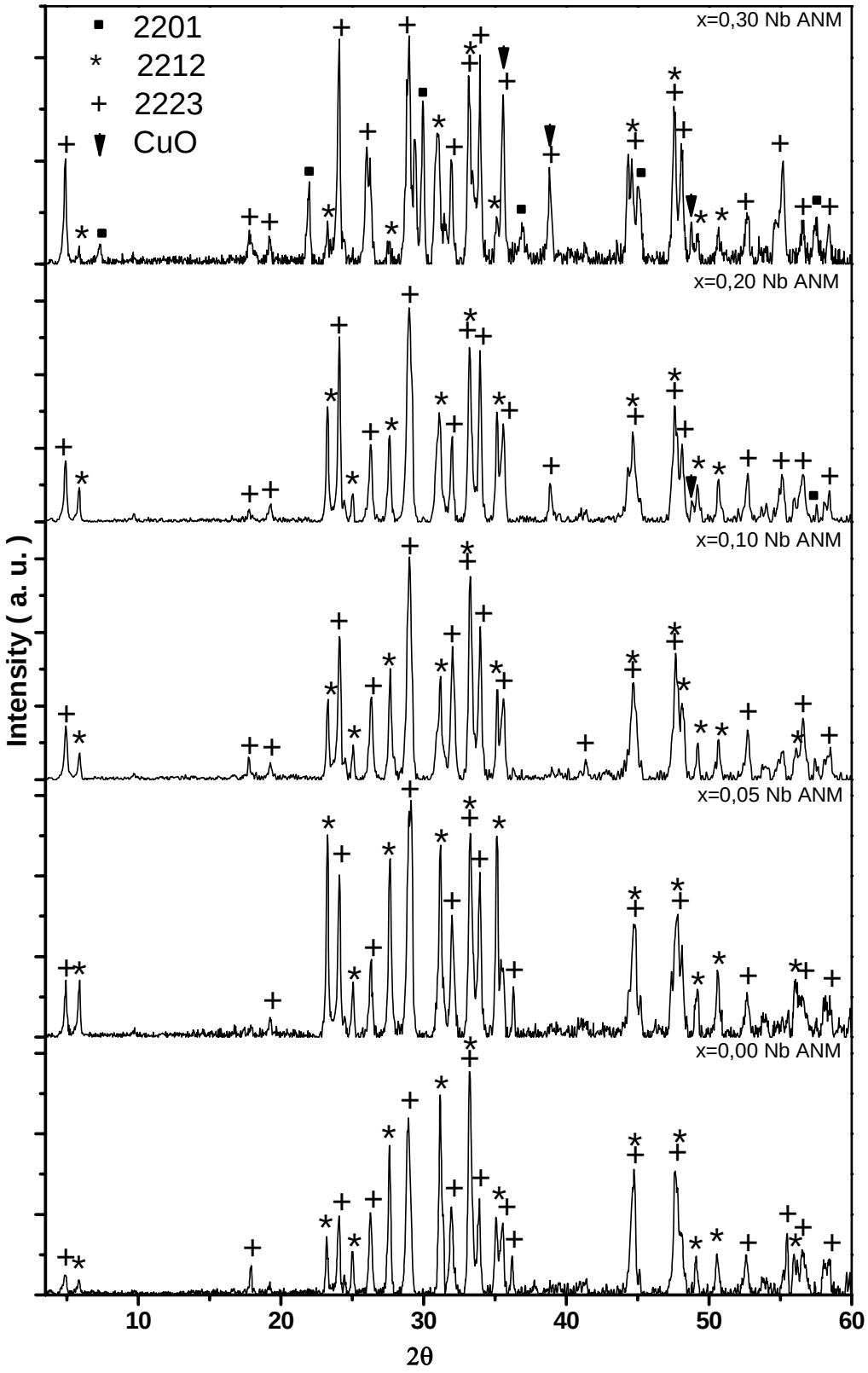

Figure 4.2 XRD patterns of samples prepared with ANM method

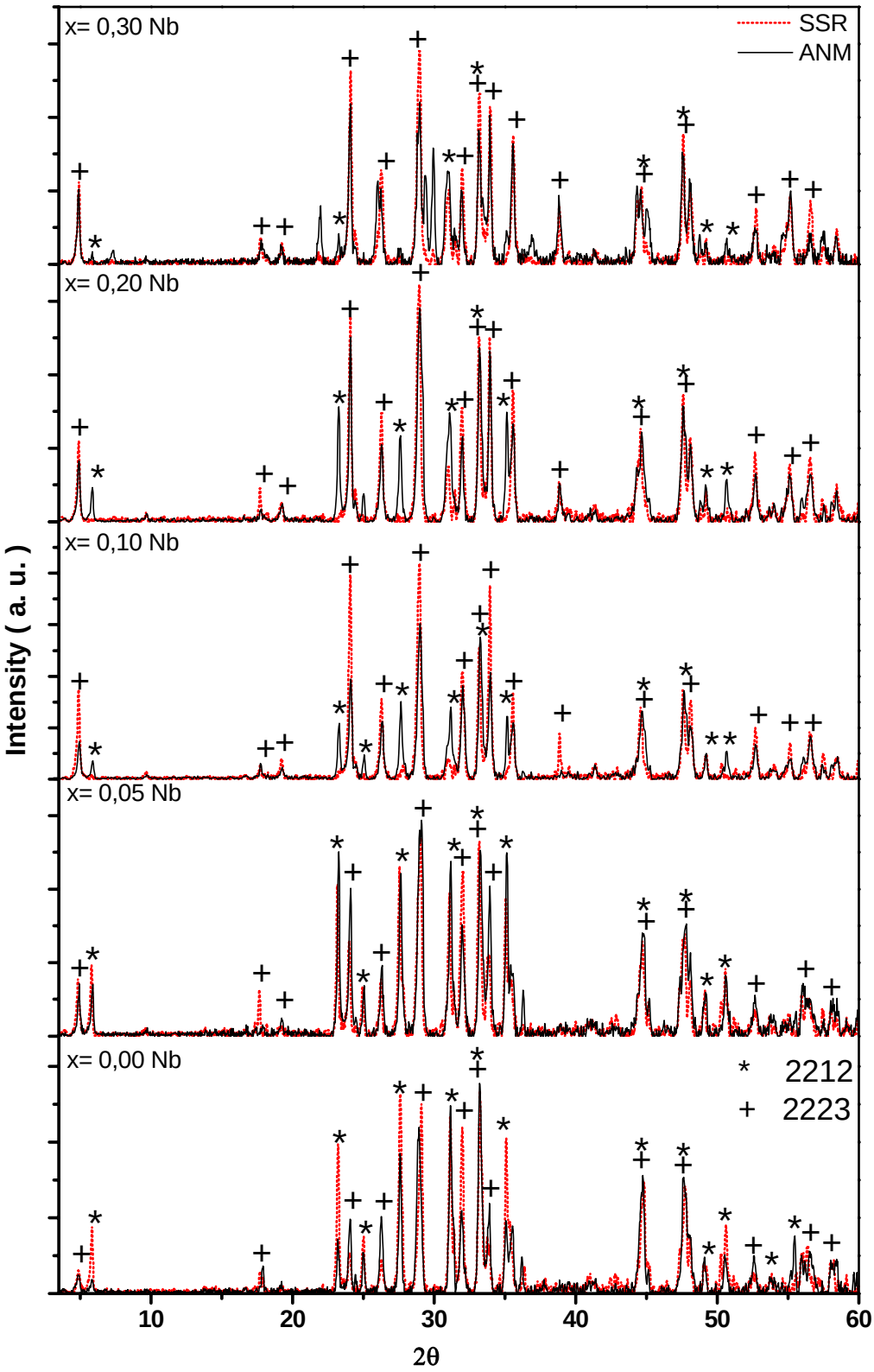

Figure 4.3 Comparative XRD patterns of both series of samples

4.3.3 Transition Temperature Measurements

The zero resistance transition temperatures were determined from the Resistance versus temperature graphs. The resistance versus temperature graph usually shows a sharp rise in resistance by increasing temperature above T_c, and then exhibits a linear increase with temperature. Results reveal higher T_c values for Nb-free sample prepared by ANM route. However, For the ANM samples the T_c changes little up to x= 0.10 and then rapidly decreases by increasing Nb content for x= 0.20 and x= 0.30 dropping from 108 K to 100 K and then below 77 K. It is suggested that Nb_2O_5 addition may affects the Cu-O planes, as these planes are very sensitive to disruptions [26]. For the case of SSR samples, T_c first increases by about 8 K (for x= 0.10 and x= 0.20) which may be caused by the excess oxygen induced in these samples. It is known that excess oxygen may act as dopant to increases the number of sites for electrons to reside and this creates hole-carriers in the crystal [26]. T_c offset versus Nb concentration, and the resistance versus temperature graphs of samples are shown in Figure 4.4 and Figure 4.5, respectively. Among the SSR samples the one with x= 0.10 has the highest T_c and this sample is a pure Bi-2223 phase. Thus x= 0.10 is the optimum amount to be added to obtain pure Bi-2223 phase with the SSR method. Similar statement can not be made for the ANM samples as there are no differences in transition temperatures and the volume fractions of high T_c phases.

The zero resistance onset temperatures were determined by calculating derivatives of resistance versus temperature graphs. The results are listed in Table 4.4 and the graphs are illustrated in Appendix B. It is seen that resistance in both Nb-free samples starts to drop at higher temperatures compared with the Nb added samples of their own series. It means that intra-grain superconductivity occurs at higher temperatures in Nb-free samples. It was observed from the transition temperature results that up to an optimum amount, Nb improves the formation of bulk superconductivity. For the ANM samples the onset transition temperatures sensitively decrease by increasing Nb content, dropping from 117 K for x= 0.00 (Nb-free) sample to 97 K for x= 0.30. For the case of SSR samples the onset transition temperature changes little, from 109 K for x= 0.00 to 106 for x= 0.30.

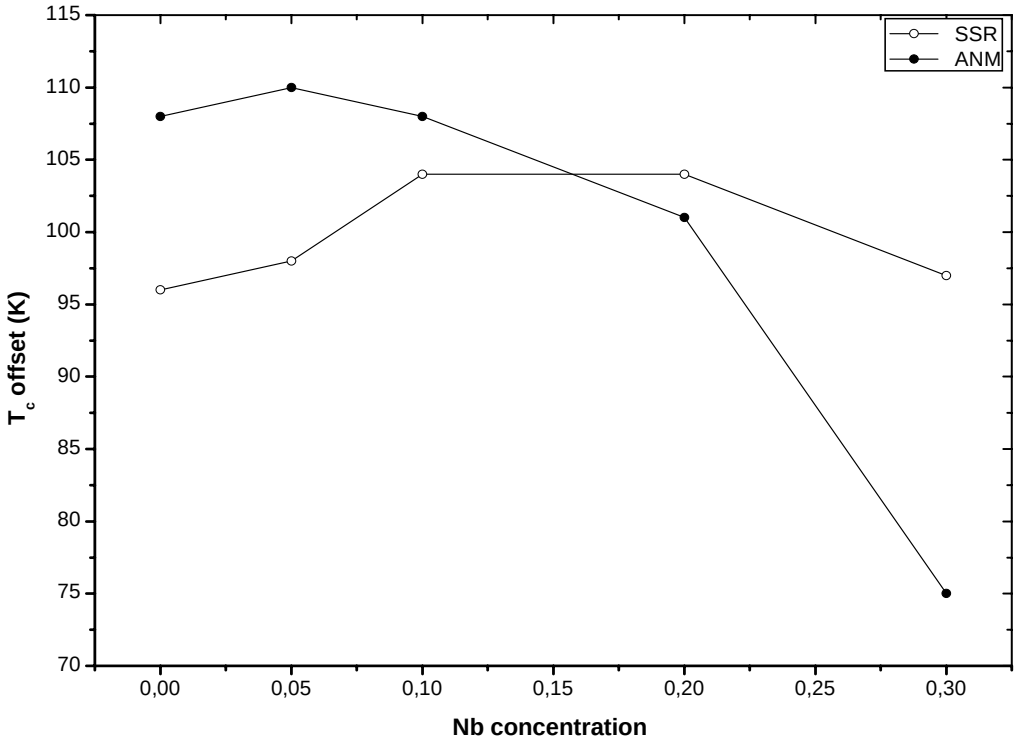

Figure 4.4 T_c offset versus Nb concentration graphs for SSR and ANM samples

Table 4.4 T_c's and onset transition temperatures for the SSR and ANM samples

	SSR		ANM	
Nb content	T_c (K)	onset transition T (K)	T_c (K)	onset transition T (K)
x= 0.00	96	109	108	117
x= 0.05	98	106	110	116
x= 0.10	104	108	108	112
x= 0.20	104	108	101	106
x= 0.30	97	106	75	97

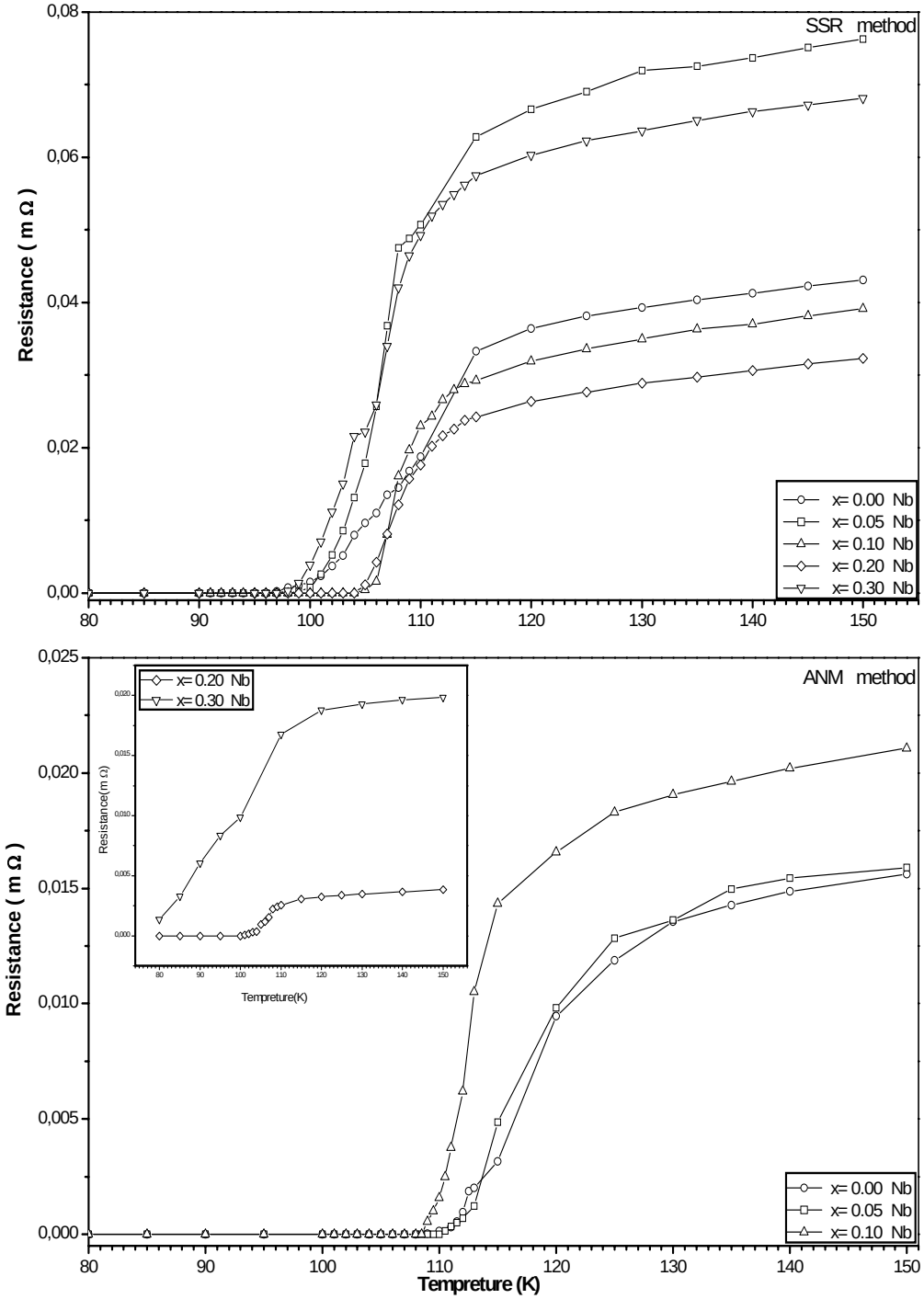

Figure 4.5 Resistance versus temperature plots for both series of samples

4.3.4 I-V Characterizations

For both SSR and ANM samples, I-V characterizations were measured at different temperatures near T_c, and the critical currents were determined. To obtain the critical current at a temperature, a DC current was applied and gradually increased until a voltage was detected. I_c values were determined between 90-110 K with 1 K intervals. The critical currents of The SSR and ANM samples are listed in Table 4.5 at 100 K. Figure 4.6 shows the I_c versus temperature graphs for the samples prepared by ANM and SSR methods. Results reveal that critical currents of the ANM samples with x= 0.00 and x= 0.05 are quit similar to each other, but increase of Nb content decreases the critical current. On the other hand, critical currents of the SSR samples increase with increase of Nb content. The increase for the samples with x= 0.10 and 0.20 is very remarkable. For example, at 102 K the I_c values of these samples are about 100 mA higher than corresponding values for the Nb-free sample. This may be due to the increase of charge carriers caused by the excess oxygen atoms gained during Nb addition [26].

Table 4.5 I_c of The SSR and ANM samples at 100 K

NB CONCENTRATION	I_C (MA) SSR	I_C (MA) ANM
x= 0.00	1.8	Above 100
x= 0.05	7.5	Above 100
x= 0.10	Above 100	97
x= 0.20	Above 100	Non-superconducting
x= 0.30	1.5	Non-superconducting

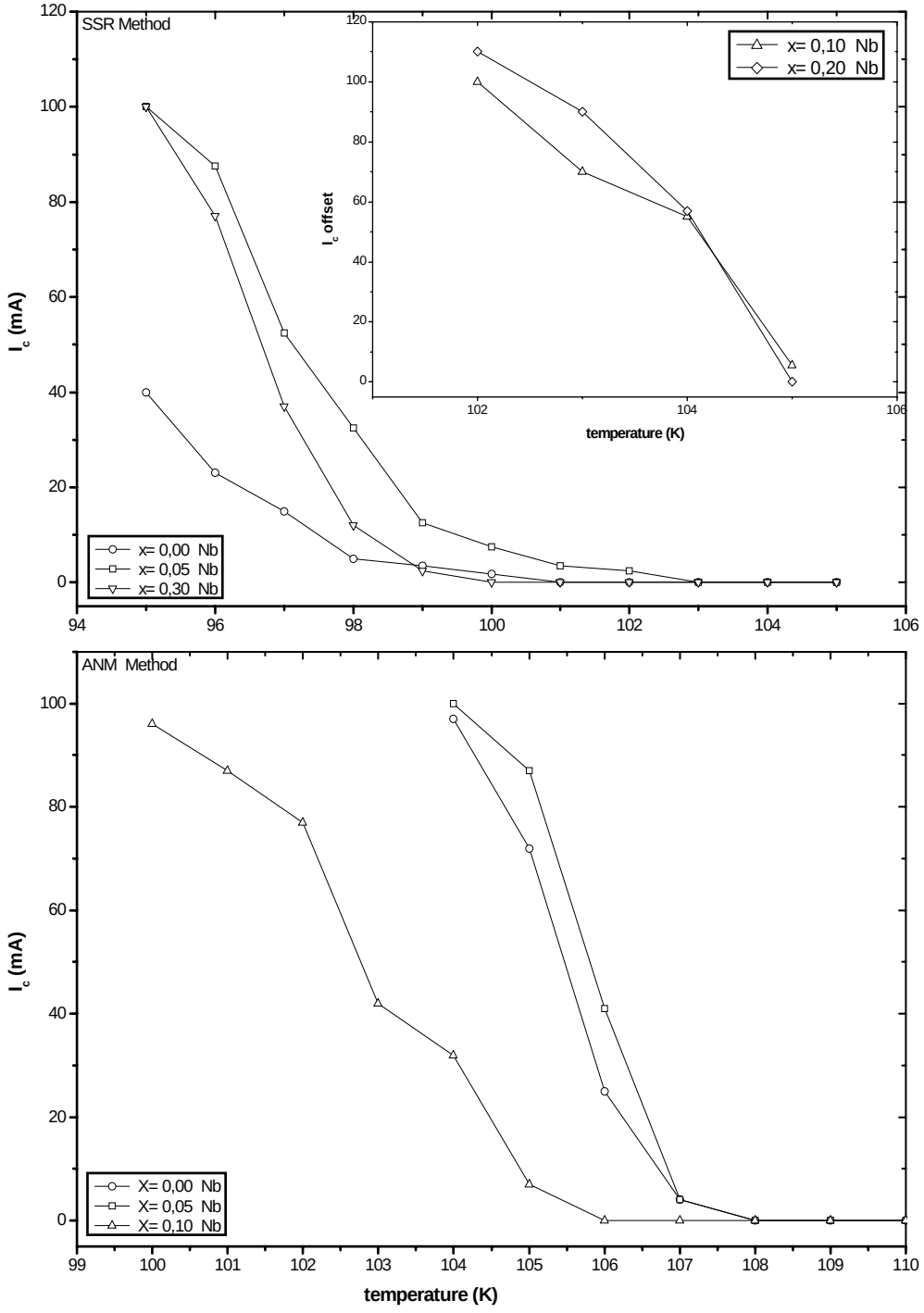

Figure 4.6 I_c offset versus temperature for the SSR and ANM samples

4.3.5 AC Susceptibility Measurements

The slope of magnetization (M) versus magnetic field is called magnetic susceptibility, χ. By applying a periodic magnetic field the AC susceptibility is measured. In general AC susceptibility is a complex quantity, expressed as $\chi = \chi' + i\chi''$, where, χ' and χ'' are the real and imaginary parts, respectively.

AC susceptibility measurement is widely used as a nondestructive method for determination and characterization of the inter-grain and intra-grain features of superconductors [18-20]. Previous studies indicate that, the real component of AC susceptibility shows two significant drops as the temperature decreased below T_c for granular superconductors. The sharp drop near T_c, corresponds to intrinsic properties of grains. The second drop at low-temperatures indicates granular changes associated with of bulk superconductivity. The imaginary component generally exhibits a peak below T_c, which is attributed to the absorption of magnetic energy from the AC field. Therefore, χ' is proportional to an amount of flux penetration into the superconductor, while, χ'' is associated with AC losses in the mixed state of superconductor.

The real and imaginary parts of the AC susceptibility for both SSR and ANM series of samples were measured by applying four different AC magnetic field, H_{AC}= 20, 40, 80, and 320 A/m and between 45-115 K. All the measurements reported here are normalized to the value of χ' at 45 K for H_{AC}= 20 A/m. The normalized AC susceptibility versus temperature graphs of the pure and Nb added samples for two series are illustrated in Figures 4.7. As the temperature decreases a two-step decrease in χ' graph is observed for all samples. The Nb added SSR samples show rather sharp inter-grain transition while Nb-free sample has a broad transition. The sharpest transition is seen for x= 0.10, the transition become broader with increase of Nb up to x= 0.30. The observations show that Nb addition improves the inter-grain coupling. The imaginary component of AC susceptibility, χ'', shows “bell-shaped” dependence on temperature. The peaks of χ'' versus temperature have shifts to higher temperatures with increase of Nb. The shifts indicate that AC loses in these samples start at higher temperatures. AC susceptibility measurements reveal that Nb added

SSR samples exhibit better superconducting properties. For the case of ANM samples, the inter-grain transitions for the first three samples, x= 0.00, 0.05 and 0.10, are sharper than the transition for last two samples, suggesting that Nb addition does not improve the transition. Also the peaks in χ'' versus temperature graph exhibits no shifts for first three samples, but for the samples with x= 0.20 and x= 0.30 peaks shift to lower temperatures. This means that AC losses start at lower temperatures for the last two samples.

The intergranular critical current density can be determined by the Bean's model [18] using

$$J_c(T_p) = H_\alpha / R \approx H_\alpha / \sqrt{ab} \qquad 4.3$$

where 2a*2b is the cross-section of the samples and H_α is related to the applied AC field. As mentioned before, χ'' versus T plots exhibits a peak at lower temperatures, T_p, corresponding to coupling between grains. The amplitude of the AC field at these temperatures is sufficiently large enough to penetrate to the center of the samples. When $H_{AC}= H_p$ the full flux penetration occurs. The H_p and T_p values were determined from the imaginary part of AC susceptibilities given in Appendix C. Figure 4.8 shows J_c versus peak temperature graphs for the SSR and the ANM samples. Also the inserted graphs display the temperature dependence of the penetration field, H_p. The observations indicate enhancement in J_c for Nb added SSR samples. Critical current densities of samples with x= 0.10 and x= 0.20 are obviously seen to be high compared with Nb-free sample. For the case of ANM samples J_c dose not change for first three samples, but decreases sharply for x= 0.20 and x= 0.30, as expected.

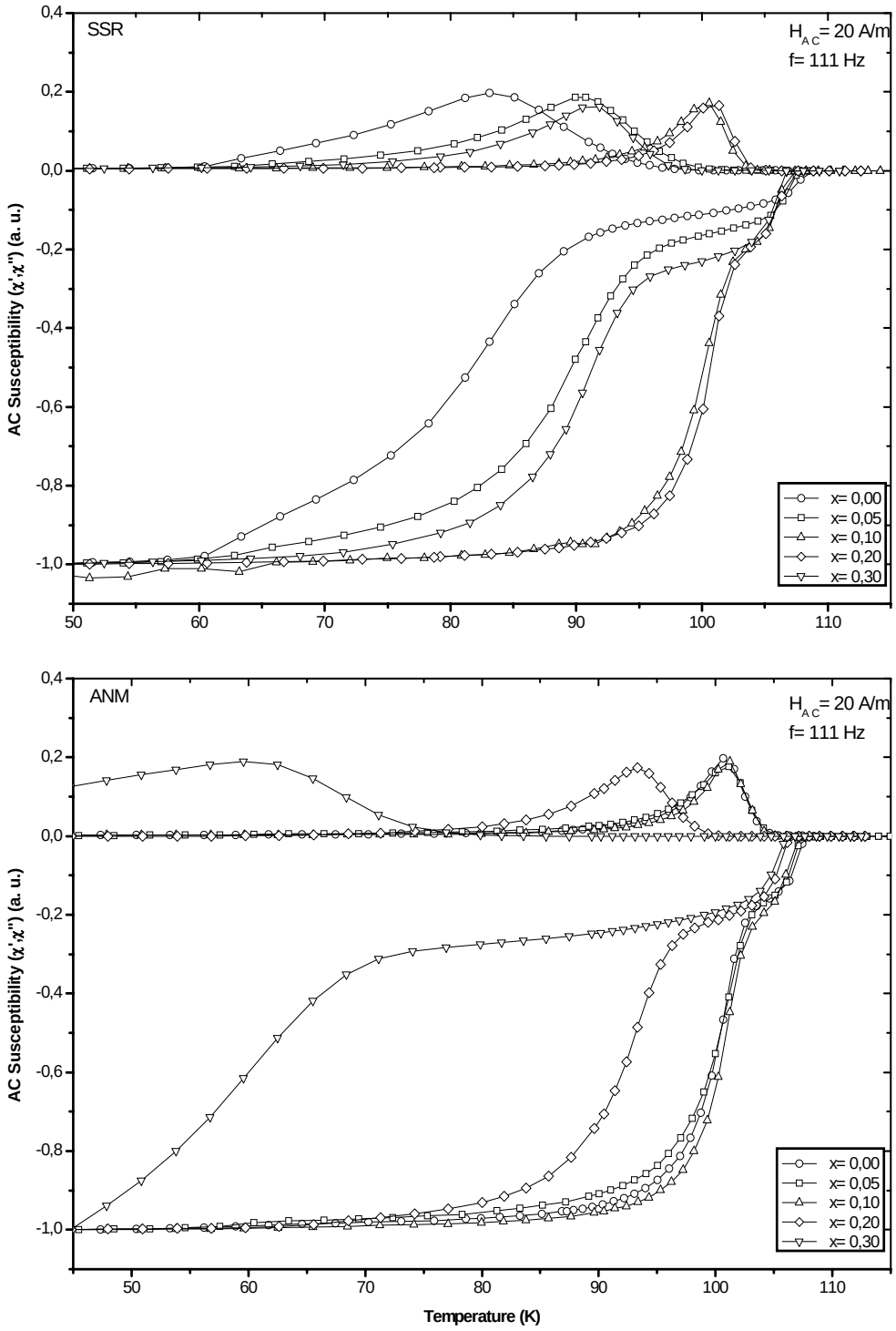

Figure 4.7 The Normalized AC susceptibility vs. temperature for SSR and ANM Samples

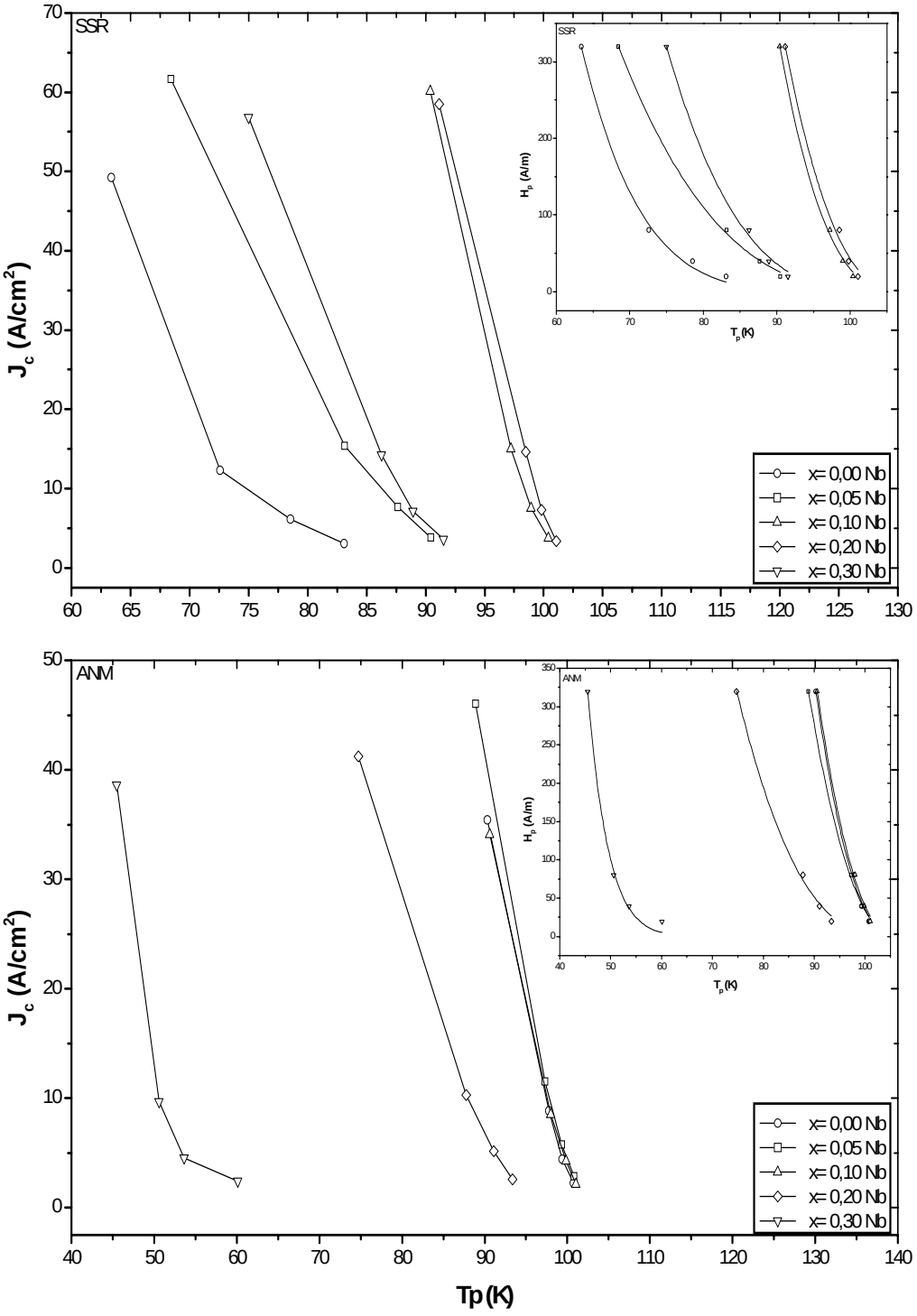

Figure 4.8 J_c vesus T_p for the SSR and ANM samples

The slopes of the real part of AC susceptibility versus temperature graphs (d χ′/dT vs. T) were evaluated. The dχ′/dT versus T graphs are shown in Figure 4.9. The peaks displayed in the graphs represent intra-grain and inter-grain transition temperatures. The intra-grain transition temperatures are determined to be about 106 K for the ANM samples. The inter-grain transition temperatures of the ANM samples are about 100-101 K for samples with x= 0.00, 0.05 and 0.10, but there is a drastic decrease in this transition to 93 and 60 K for the samples with x= 0.20 and x= 0.30, respectively. For the case of SSR samples, the intra-grain transition temperatures are about 106 K as in the ANM samples. The inter-grain transition temperature of the SSR samples were determined as 84, 91, 100, 100, and 91 K for x= 0.00, 0.05, 0.10, 0.20, and 0.30, respectively. These results suggest that x= 0.10 for the ANM route and x= 0.20 for SSR route are the optimum Nb content to obtain High T_c.

Table 4.6 Inter-grain and intra-grain transition temperatures

SAMPLES	T_C (K)			
	intra-grain ANM	**inter-grain ANM**	**intra-grain SSR**	**inter-grain SSR**
x=0.00	106.76	100.71	107.70	83.24
x=0.05	106.14	101.10	106.44	91.30
x=0.10	106.08	101.30	106.29	100.47
x=0.20	105.17	93.26	106.25	100.70
x=0.30	104.86	59.90	105.23	91.27

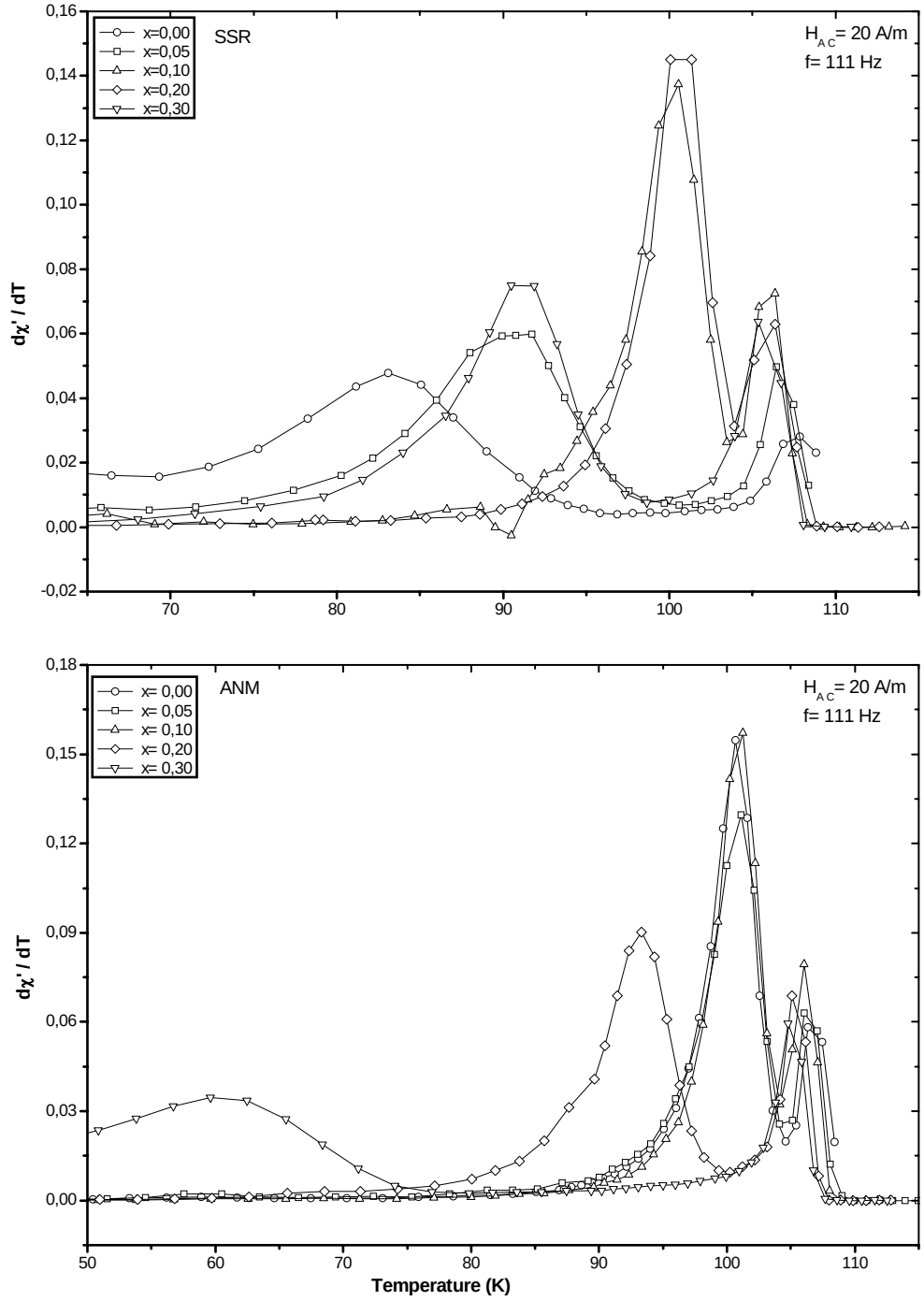

Figure 4.9 Derivatives of the χ′ versus temperature for SSR and ANM samples

4.3.6 Inductive Critical Current Density Measurements

Inductive critical current densities of the samples were also calculated using the Bean Model [18] from the magnetization measurements. The measurements were carried out at 50 K and 77 K. Critical currents versus Nb content are plotted in Figure 4.10. This measurement along with I-V characterizations indicate a very important result of this research, which is the noticeable increase in J_c values for the samples with x= 0.10 and x= 0.20 prepared by SSR method. For x= 0.10, a pure Bi-2223 phase were obtained. The increase in J_c may be caused by increase of charge carriers. For the sample with x= 0.20 the presence of low amount of Bi-2212 phase may act as pinning centers for vortices [23]. For the ANM samples there is a minor increase in J_c for x= 0.05 and then it starts to decrease with increase of x. In ANM method more homogeneous samples having smaller grains are produced. Smaller grains means more grain boundaries and weak link. Nb addition may further increase the grain boundaries and at the same time may degrade the Cu-O planes. These may be the reason for the decrease of J_c with increase of Nb content for the ANM samples.

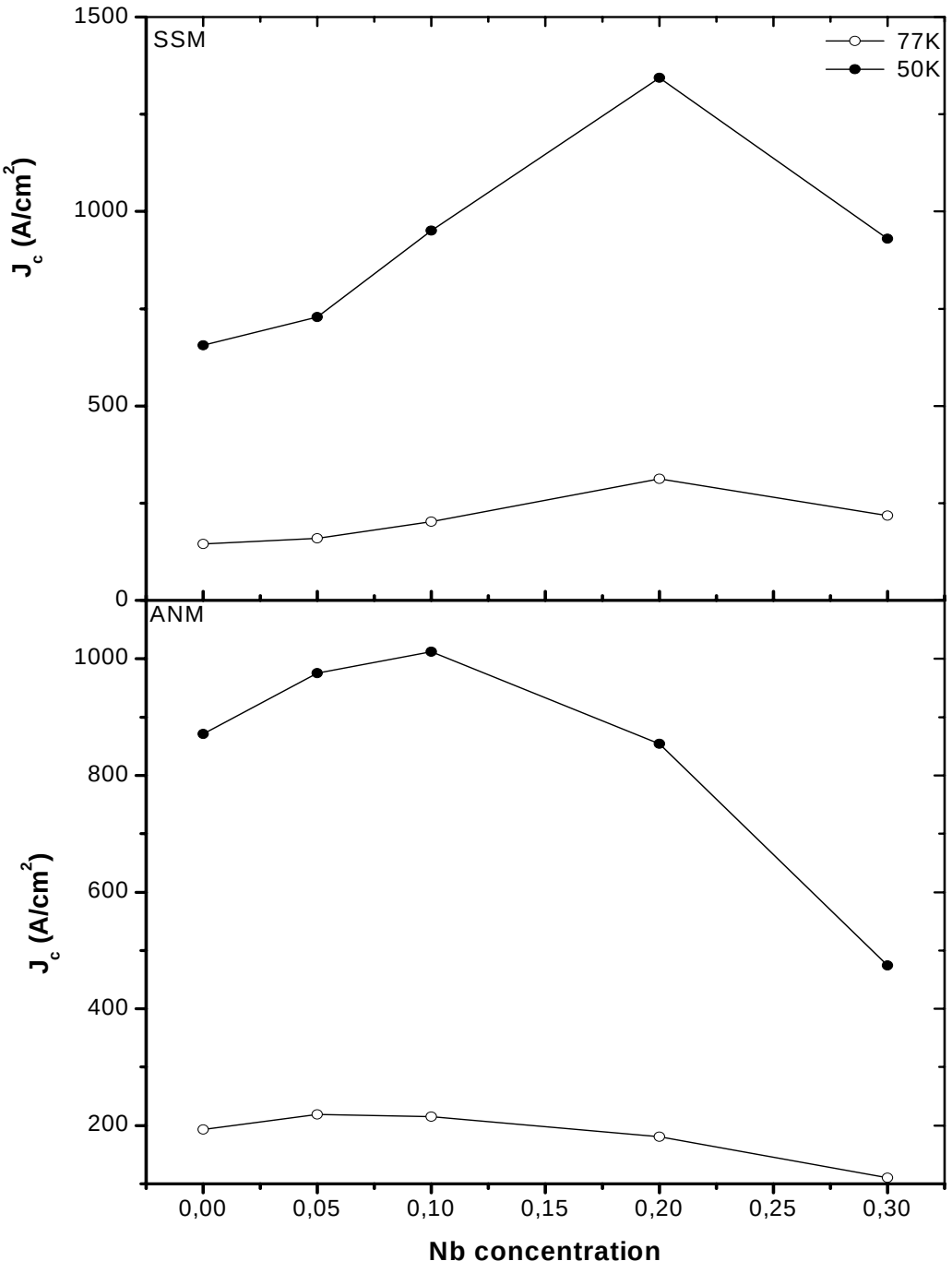

Figure 4.10 J_c versus Nb concentration for SSR and ANM samples

4.3.7 SEM Analysis

Figure 4.11 displays surface micrographs of the Nb-free samples of SSR and ANM series. It is seen that the grains of SSR sample are larger than the grains of ANM sample. This is the characteristic of ANM route; growth samples with fine grains.

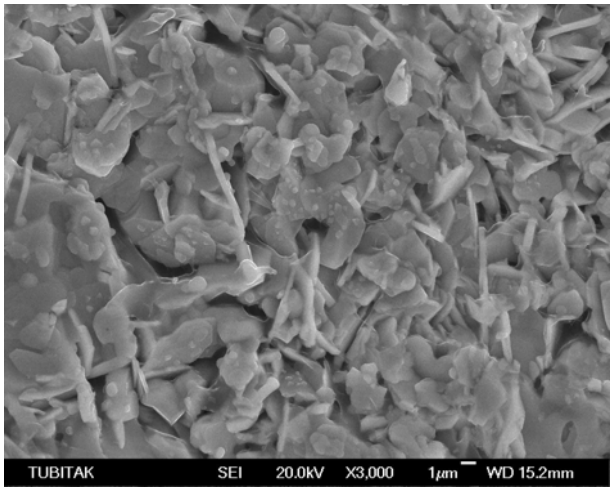

x= 0.00 SSR

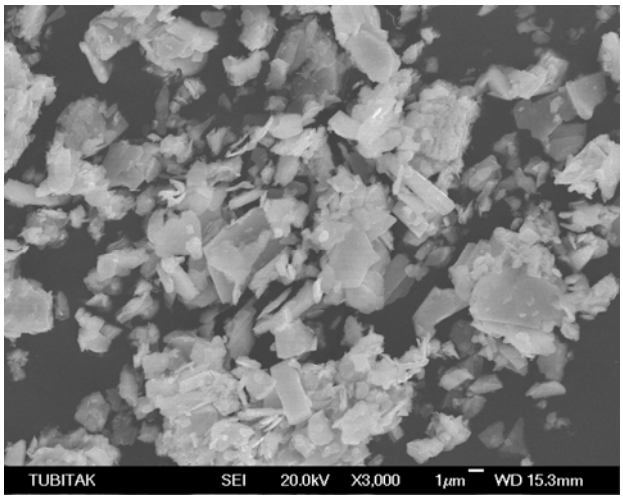

x= 0.00 ANM

Figure 4.11 SEM photographs of the Nb-free SSR and ANM samples

CHAPTER 5

CONCLUSION

Two series of samples having chemical composition of $Bi_{1.6}Pb_{0.4}Sr_2Ca_2Cu_3Nb_xO_y$ were sintered using two different methods, solid state reaction and ammonium melt methods, with Nb concentration varying from x= 0.00 to x= 0.30. XRD measurements reveal that the volume fraction of Bi-2223 phase is higher in the ANM sample compared to SSR one for x= 0.00. As a result, T_c, and J_c of the ANM sample without Nb is higher. For the ANM samples the volume fraction of Bi-2223 does not change much with Nb addition, but Nb addition enhances the high-T_c phase formation of the samples prepared in SRR route. The reason for the better superconducting properties for Nb-free ANM sample may be the higher oxygen content of the samples prepared by ANM route. EDX analysis of Nb-free sample sintered by ANM also showed higher oxygen concentration.

Nb_2O_5 addition strongly improves high-T_c phase formation, T_c and J_c in the SSR samples. Almost pure Bi-2223 phase was obtained with the SSR method for x= 0.10. Based on this observation it is suggested that Nb behaves as Pb to stabilize the formation of Bi-2223 [23]. J_c of the SSR sample with x= 0.20 is quit high. This sample contains about 5 % Bi-2212 phase. The increase of J_c may be partially caused by Bi-2212 phase behaving as pining centers. ANM samples also show slight improvement in T_c and J_c with small amount of Nb addition. Based on all these observations, optimum Nb concentration can be expressed by the composition $Bi_{1.6}Pb_{0.4}Sr_2Ca_2Cu_3Nb_{0.10}O_y$.

AC susceptibility measurements also support the results obtained from XRD, T_c, and J_c measurements. Intra and inter-grain transition temperatures, interaction between grains and J_c obtained from AC susceptibility all indicate the improvements reported in this study. Overall, present study indicates that for both series of samples, ANM and SSR, better superconducting properties can be obtained with Nb addition up to optimum levels.

REFERENCES

[1] H. Kamerling Onnes, Commun. Phys. Lab. Univ. Leiden 124c (1911)

[2] W. Meissner and R. Ochsenfeld, Naturwissenschaften 21, 787 (1933)

[3] L. W. Schubnikow and I. E. Nakhatin, Nature 139, 589 (1937)

[4] E. Maxwell, Phys. Rev. 78, 477 (1950)

[5] A. Reynolds, B. Serin, W. H. Wright, and L. B. Nesbitt, Phys. Rev. 78, 478 (1950)

[6] J. Bardeen, L. N. Cooper, and J, R, Schrieffer, Phys. Rev. 108, 1175 (1957)

[7] J. G. Bednorz and K. A. Muller, Z, Phys. B 64, 189 (1986)

[8] M. K. Wu, J. R. Ashburn, C. J. Torng, P. H. Hor, R. L. Meng, L. Gao, Z. J. Huang, Y. Q. Wang, and C. W. Chu, phys. Rev. Lett., 58, 908, 911 (1987)

[9] Raveau et. al., Physical Review B, (1987)

[10] H. Maeda, Y. Tanaka, M. Fukutomi, and T. Alonso, Japan. J. Appl. Phys., 27, 209, (1988)

[11] Z. Z. Sheng and A. M. Hermann, Nature 332, 55 (1989)

[12] A. Schilling et al., Nature 363, 56 (1993)

[13] H. Nasn, N. Kuriyama, K. Kamiya, Jpn. J. Appl. Phys., 29**,** 1415 (1990)

[14] Y. Li, B. Yang, J. Mater. Sci. Lett., 13**,** 594 (1994)

[15] D. Sykorova, O. Smrckova, and P. Vasek, Int. J. Mod. Phys., B 13**,** 3738-3740 (1999)

[16] D. R. Mishra, P. L. Upadhyay, R. G. Sharma, Physica C, 304**,** 293-306 (1998)

[17] T. Kanai, T. Kamo, S. P. Matsuda, Jpn. J. Appl. Phys., 28**,** 1551 (1989)

[18] Bean CP, Rev.Mod. Phys., 36, 31 (1964)

[19] Goldfarb R B, Lelental M, and Thompson, AC Magnetic Susceptibility of Superconductors and Other Spin Systems (New York: Plenum) (1992)

[20] D-X. Chen, Yu Mei, and H. L. Luo, Physica C, 167**,** 317-323 (1990)

[21] Salahattin Celebi, Physica C, 316, 251-256 (1999)

[22] Vlademir Z. Kresin, and Stuart A. Wolf, Fundamentals of Superconductivity, (New York: Plenum) (1990)

[23] Hiroshi Maeda, and Kazumasa Togano, Bismuth-based High-Temperature Superconductors (1996)

[24] Zhi-Xiong Cai, and Yimei Zhu, Microstructures and Structural Defects in High-Temperature Superconductors (1998)

[25] Andrei Mourachkine, High-Temperature Superconductivity in Cupates (2002)

[26] Anderi Mourachkine, Room-Temperature Superconductivity (2004)

[27] Thomas P. Sheahen, Introduction to High-Temperature Superconductivity (1994)

APPENDIX A

Table A.1 Composition of the samples from EDX analysis

Element	Weight %	Atomic %
O K	14.45	49.22
Ca K	7.41	10.08
Cu K	23.99	20.58
Sr L	16.57	10.31
Pb M	3.84	1.01
Bi M	33.73	8.80
Totals	100.00	

x= 0.00 Nb ANM

Element	Weight %	Atomic %
O K	16.99	55.53
Ca K	6.64	8.67
Cu K	18.54	15.26
Sr L	16.46	9.82
Nb L	1.15	0.65
Pb M	7.43	1.87
Bi M	32.79	8.21
Totals	100.00	

x= 0.05 Nb ANM

Element	Weight %	Atomic %
O K	16.94	55.13
Ca K	6.79	8.83
Cu K	19.08	15.63
Sr L	16.25	9.66
Nb L	1.73	0.97
Pb M	6.55	1.65
Bi M	32.66	8.14
Totals	100.00	

x= 0.10 Nb ANM

Element	Weight %	Atomic %
O K	15.67	53.12
Ca K	6.52	8.82
Cu K	19.05	16.25
Sr L	16.30	10.09
Nb L	2.11	1.23
Pb M	6.47	1.69
Bi M	33.87	8.79
Totals	100.00	

x= 0.20 Nb ANM

Element	Weight %	Atomic %
O K	16.13	54.73
Ca K	6.59	8.93
Cu K	16.01	13.68
Sr L	15.64	9.69
Nb L	3.39	1.98
Pb M	5.33	1.40
Bi M	36.91	9.59
Totals	100.00	

x= 0.30 Nb ANM

Element	Weight %	Atomic %
O K	14.80	50.41
Ca K	7.39	10.05
Cu K	20.51	17.59
Sr L	19.39	12.06
Pb M	6.45	1.70
Bi M	31.45	8.20
Totals	100.00	

x= 0.00 Nb SSR

Element	Weight %	Atomic %
O K	15.00	51.45
Ca K	6.88	9.42
Cu K	20.31	17.55
Sr L	16.71	10.47
Nb L	0.95	0.56
Pb M	5.65	1.50
Bi M	34.51	9.06
Totals	100.00	

x= 0.05 Nb SSR

Element	Weight %	Atomic %
O K	18.05	53.96
Si K	3.85	6.55
Ca K	7.29	8.71
Cu K	17.96	13.53
Sr L	15.09	8.24
Nb L	1.26	0.65
Pb M	5.29	1.22
Bi M	31.21	7.14
Totals	100.00	

x= 0.10 Nb SSR

Element	Weight %	Atomic %
O K	15.56	51.24
Ca K	6.82	8.96
Cu K	25.01	20.73
Sr L	14.97	9.00
Nb L	1.81	1.03
Pb M	4.62	1.18
Bi M	31.20	7.87
Totals	100.00	

x= 0.20 Nb SSR

Element	Weight %	Atomic %
O K	16.67	53.97
Ca K	6.63	8.57
Cu K	21.20	17.28
Sr L	16.68	9.86
Nb L	2.23	1.24
Pb M	5.34	1.34
Bi M	31.25	7.74
Totals	100.00	

x= 0.30 Nb SSR

APPENDIX B

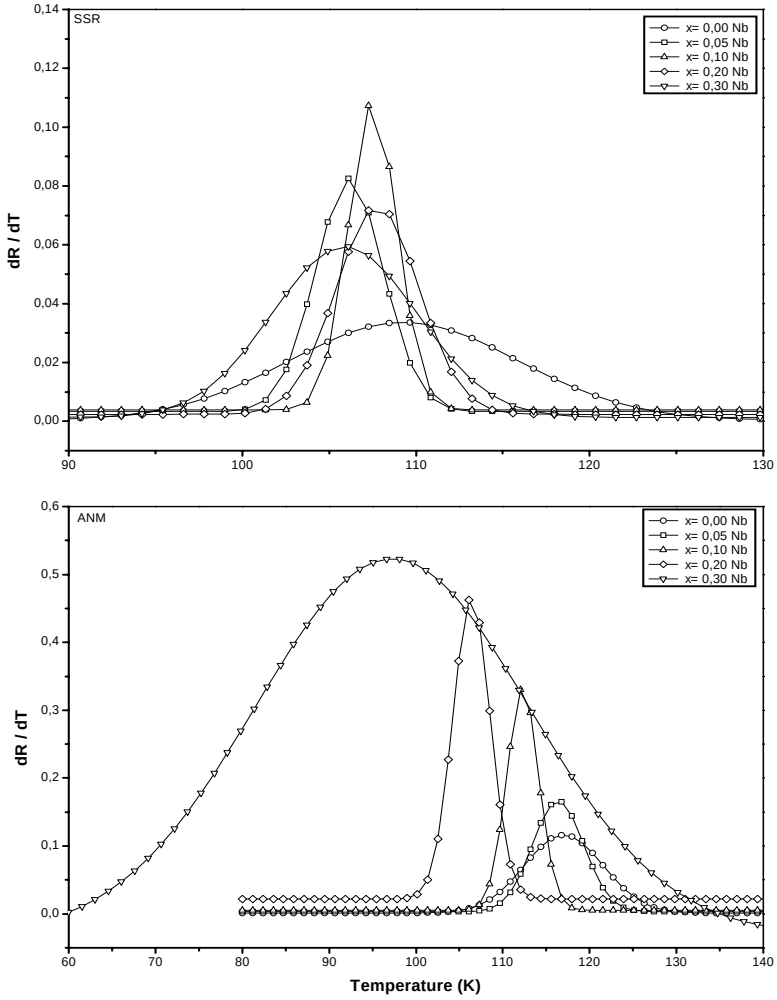

Figure B.1 dR/dT versus T plots obtained from R versus T graphs

APPENDIX C

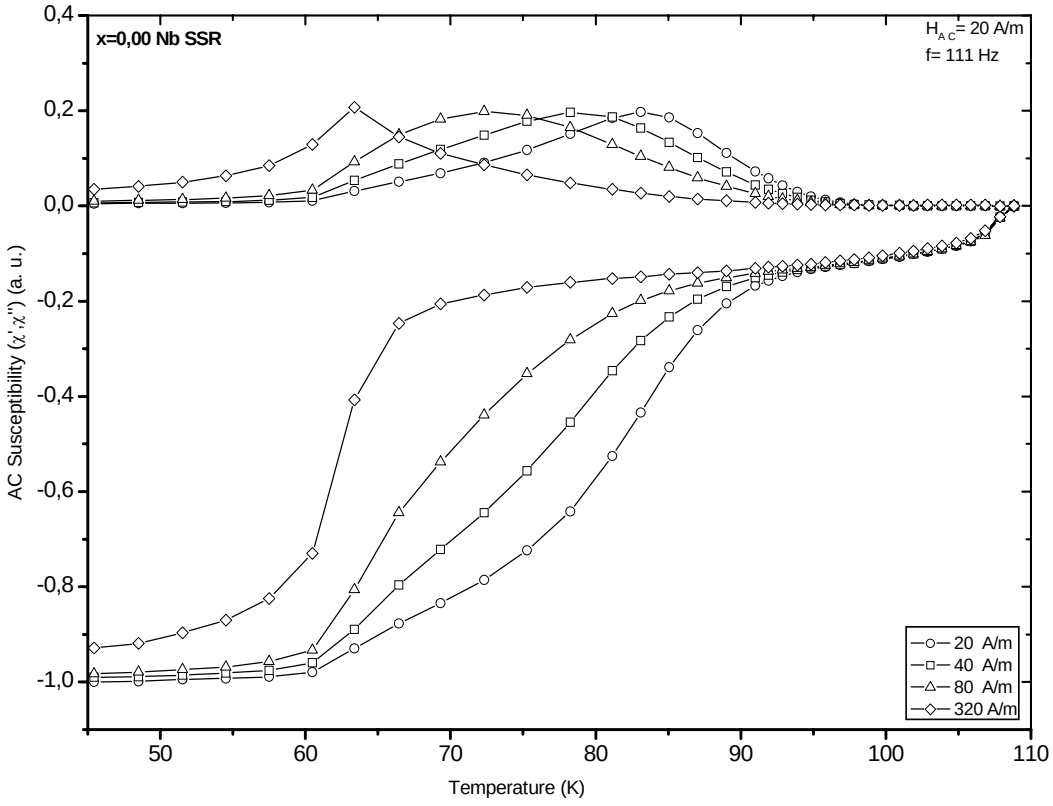

Figure C.1 AC susceptibility versus temperature graphs

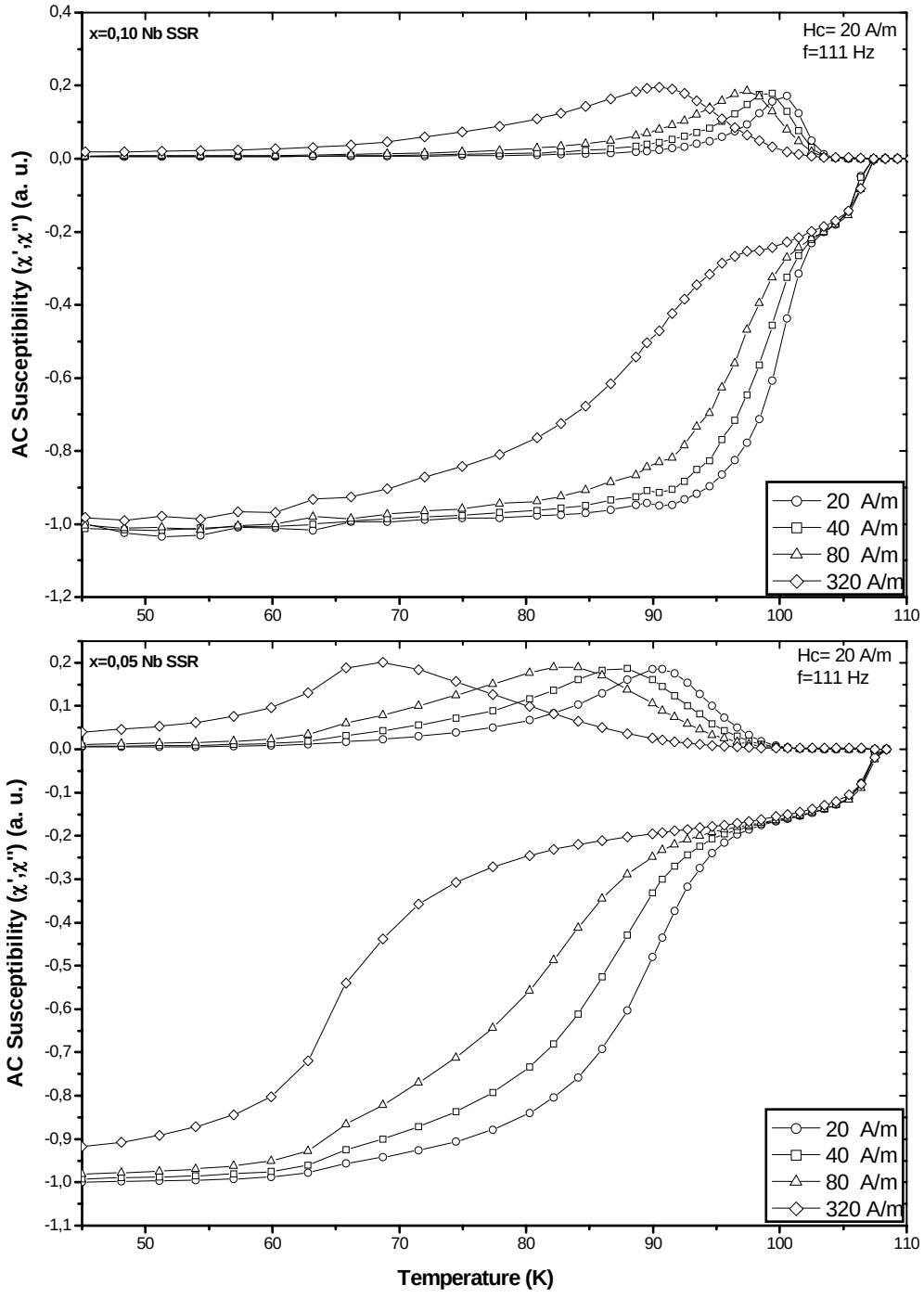
x=0,10 Nb SSR
Hc= 20 A/m
f=111 Hz
AC Susceptibility (χ',χ'') (a. u.)
20 A/m
40 A/m
80 A/m
320 A/m
x=0,05 Nb SSR
Hc= 20 A/m
f=111 Hz
AC Susceptibility (χ',χ'') (a. u.)
20 A/m
40 A/m
80 A/m
320 A/m
Temperature (K)

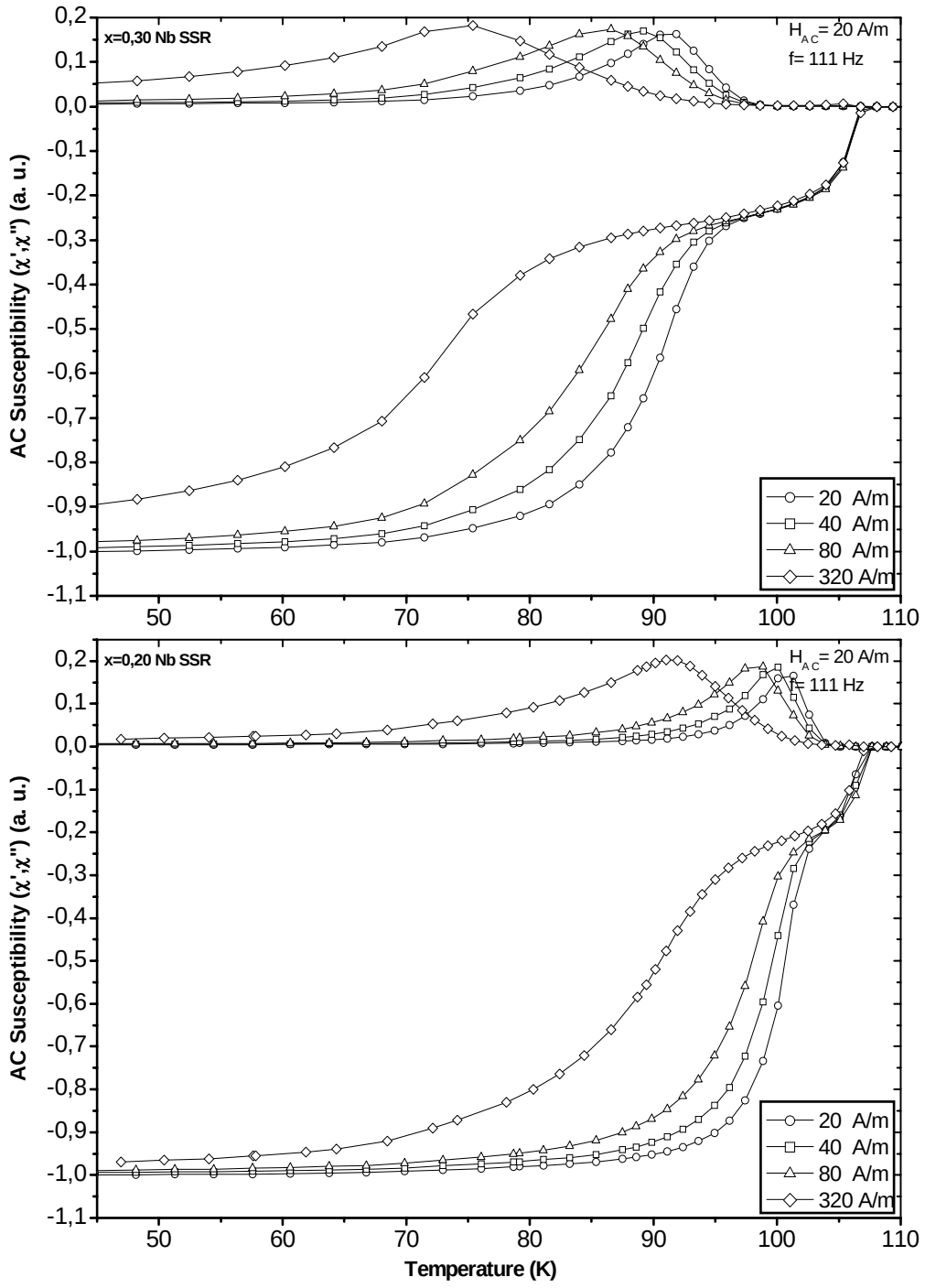
x=0,30 Nb SSR
H_AC= 20 A/m
f= 111 Hz
AC Susceptibility (χ',χ") (a. u.)
20 A/m
40 A/m
80 A/m
320 A/m
x=0,20 Nb SSR
H_AC= 20 A/m
f= 111 Hz
AC Susceptibility (χ',χ") (a. u.)
20 A/m
40 A/m
80 A/m
320 A/m
Temperature (K)

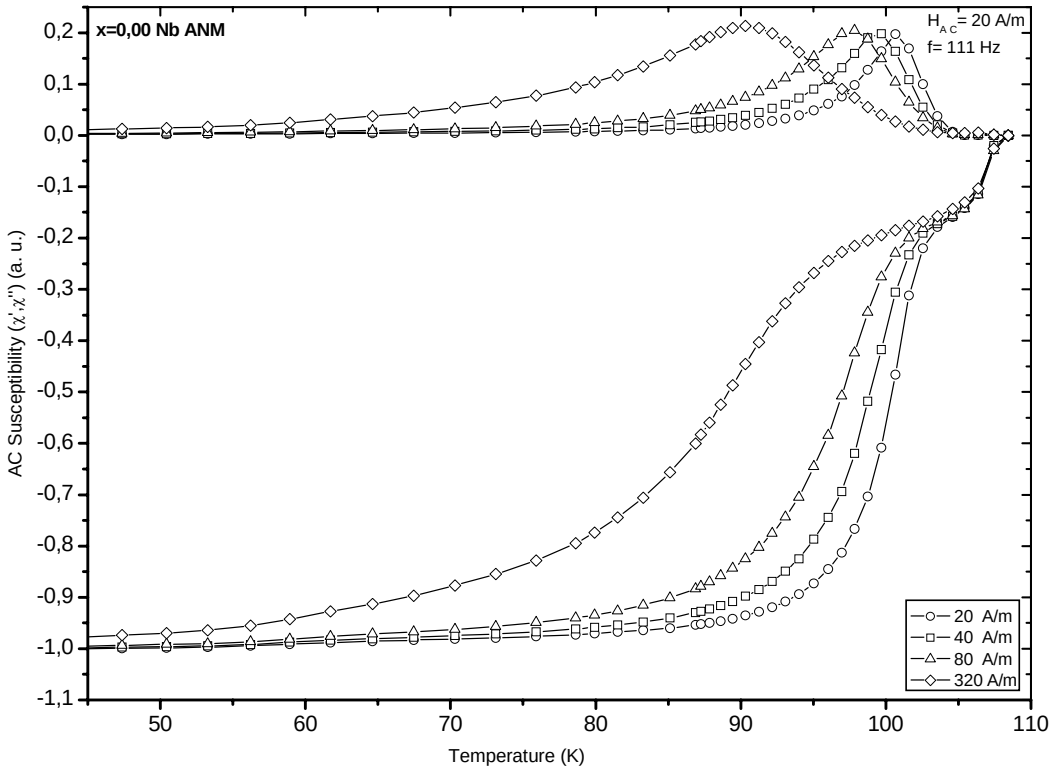
x=0,00 Nb ANM
H AC = 20 A/m
f= 111 Hz
AC Susceptibility (χ';χ'') (a. u.)
Temperature (K)
20 A/m
40 A/m
80 A/m
320 A/m

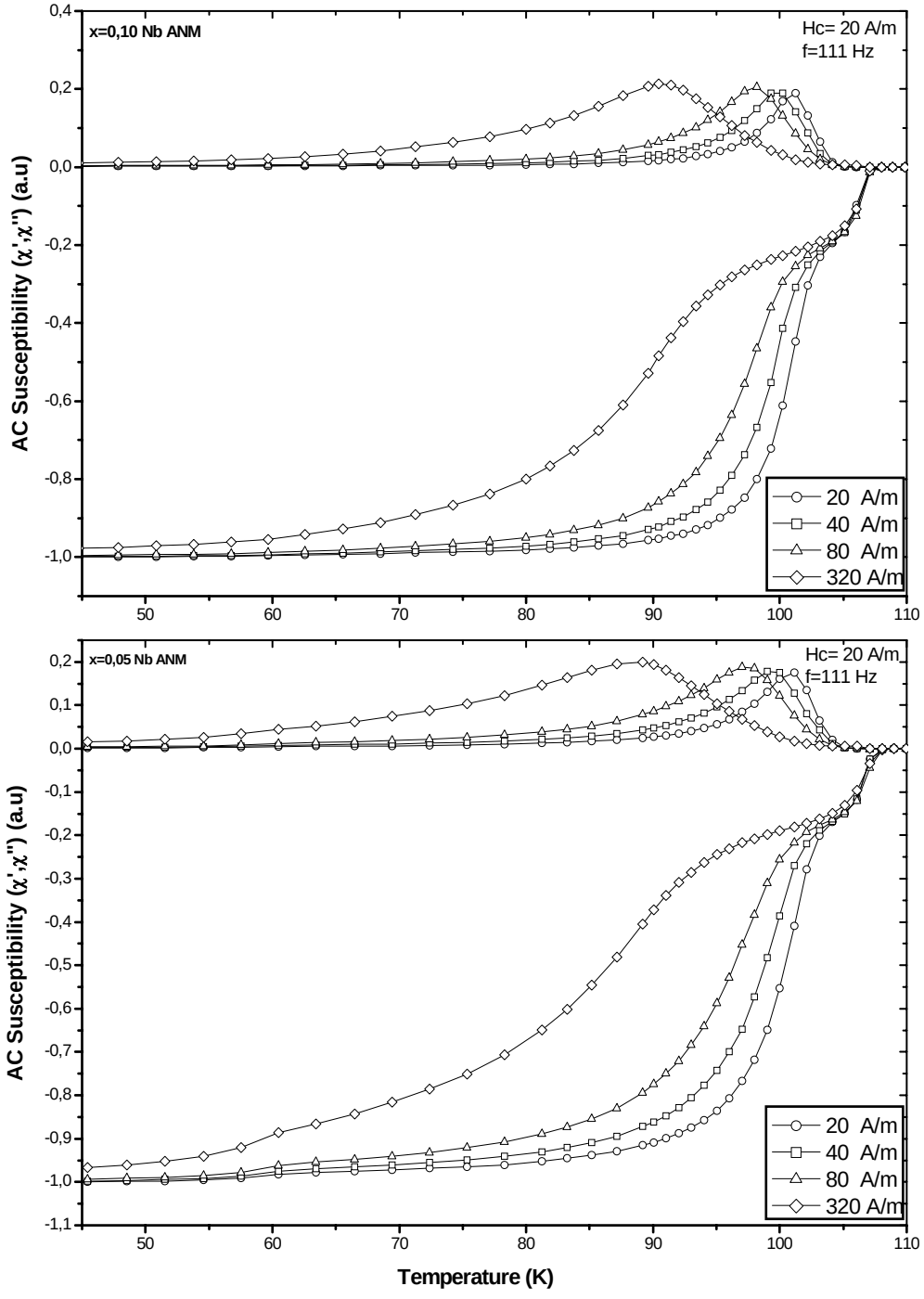
x=0,10 Nb ANM
Hc= 20 A/m
f=111 Hz
AC Susceptibility (χ',χ") (a.u)
20 A/m
40 A/m
80 A/m
320 A/m
x=0,05 Nb ANM
Hc= 20 A/m
f=111 Hz
AC Susceptibility (χ',χ") (a.u)
Temperature (K)

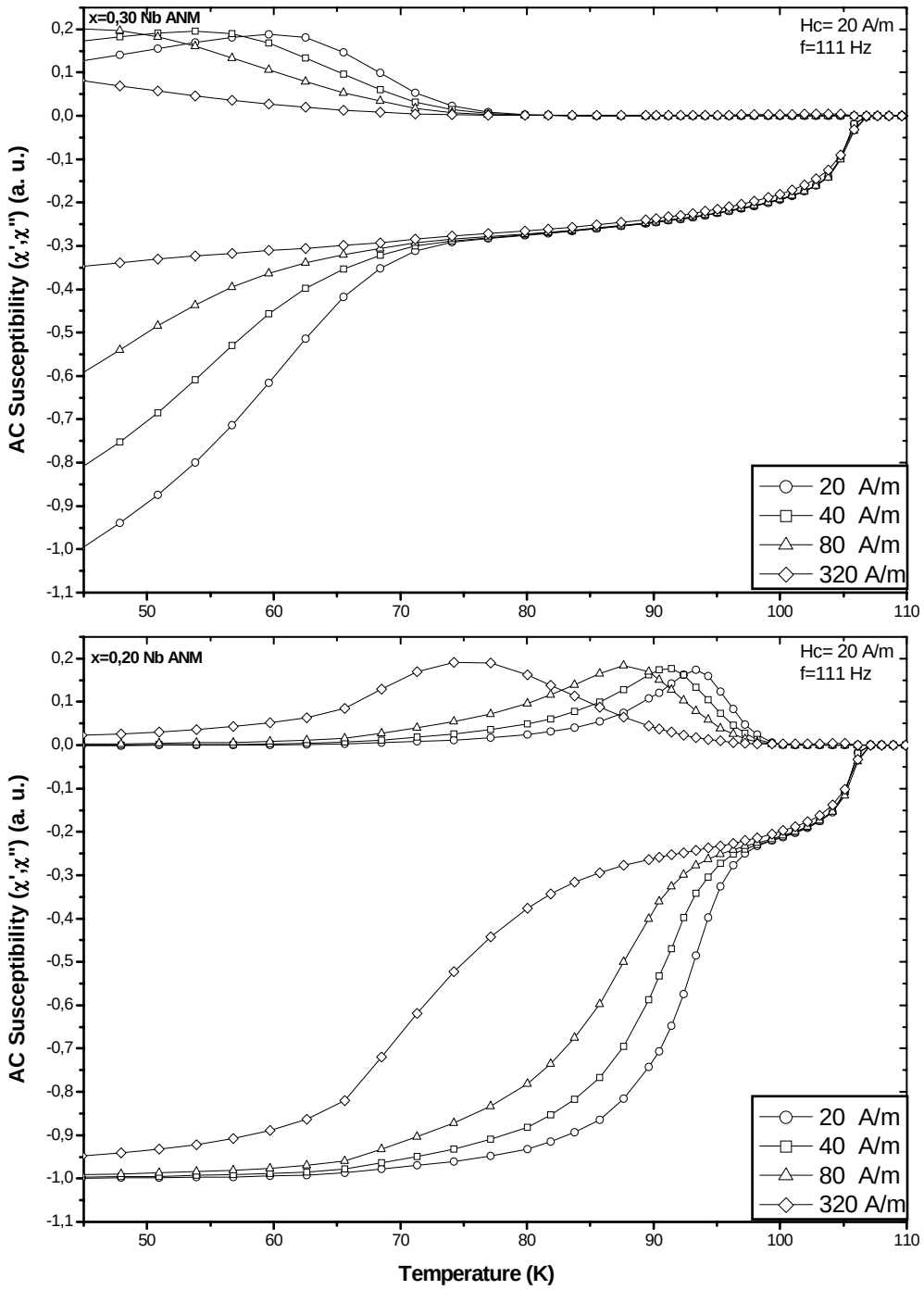
x=0,30 Nb ANM
Hc= 20 A/m
f=111 Hz
AC Susceptibility (χ',χ") (a. u.)
20 A/m
40 A/m
80 A/m
320 A/m
x=0,20 Nb ANM
Hc= 20 A/m
f=111 Hz
AC Susceptibility (χ',χ") (a. u.)
20 A/m
40 A/m
80 A/m
320 A/m
Temperature (K)

APPENDIX D

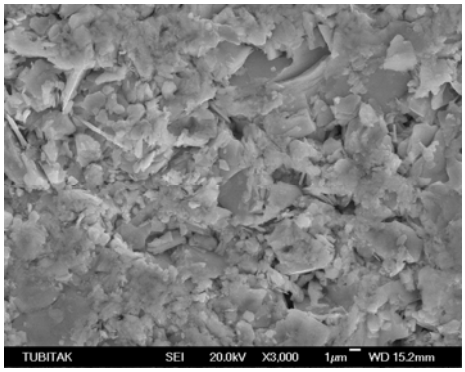

x= 0.05 Nb (SSR)

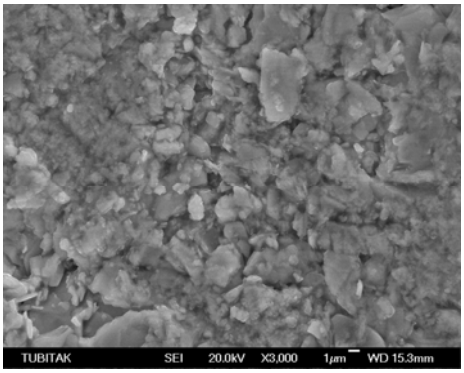

x= 0.10 Nb (SSR)

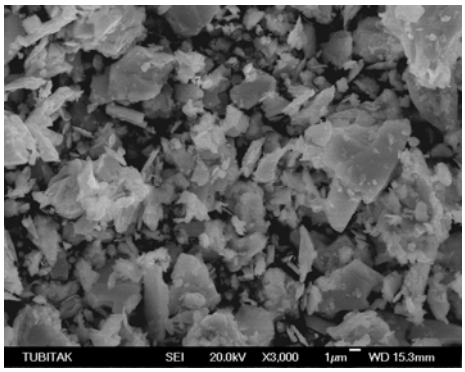

x= 0.20 Nb (SSR)

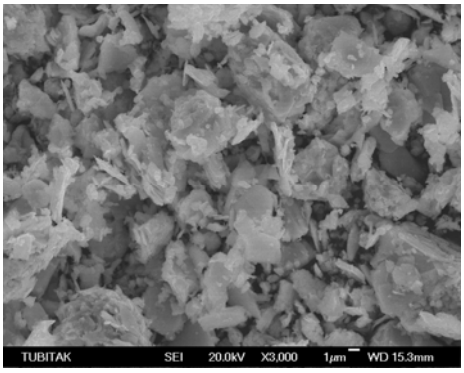

x= 0.30 Nb (SSR)

Figure D.1 Micrographs of the selected areas of the samples

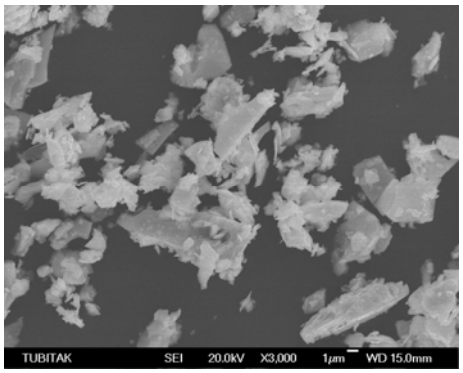

x= 0.05 Nb (ANM)

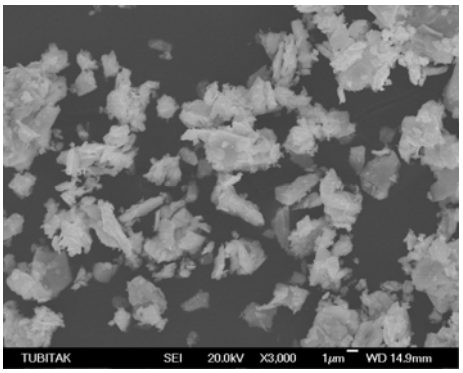

x= 0.10 Nb (ANM)

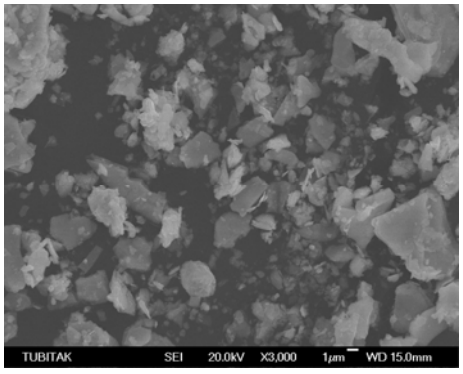

x= 0.20 Nb (ANM)

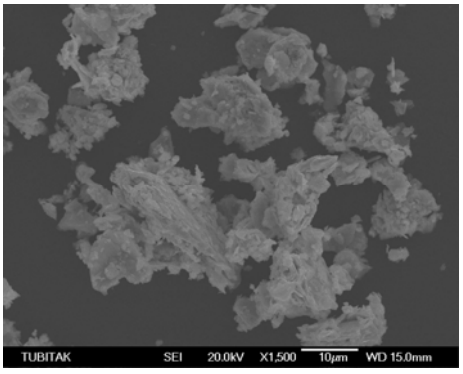

x= 0.30 Nb (ANM)